Molecular Microbiology (2013) 89(6), 1167–1186 ■
doi:10.1111/mmi.12334
First published online 15 August 2013

The *Plasmodium* translocon of exported proteins (PTEX) component thioredoxin-2 is important for maintaining normal blood-stage growth

Kathryn Matthews,[1] Ming Kalanon,[1] Scott A. Chisholm,[1] Angelika Sturm,[2] Christopher D. Goodman,[2] Matthew W. A. Dixon,[3] Paul R. Sanders,[4] Thomas Nebl,[5] Fiona Fraser,[1] Silvia Haase,[1†] Geoffrey I. McFadden,[2] Paul R. Gilson,[4] Brendan S. Crabb[4] and Tania F. de Koning-Ward[1*]

[1]*School of Medicine, Deakin University, Waurn Ponds, Vic. 3216, Australia.*
[2]*School of Botany, University of Melbourne, Melbourne, Vic. 3010, Australia.*
[3]*Department of Biochemistry and Molecular Biology, Bio21 Institute, Melbourne, Vic. 3010, Australia.*
[4]*Macfarlane Burnet Institute for Medical Research and Public Health, Melbourne, Vic. 3004, Australia.*
[5]*Infection and Immunity Division, The Walter and Eliza Hall Institute, Melbourne, Vic., 3052, Australia.*

Summary

Plasmodium **parasites remodel their vertebrate host cells by translocating hundreds of proteins across an encasing membrane into the host cell cytosol via a putative export machinery termed PTEX. Previously PTEX150, HSP101 and EXP2 have been shown to be *bona fide* members of PTEX. Here we validate that PTEX88 and TRX2 are also genuine members of PTEX and provide evidence that expression of PTEX components are also expressed in early gametocytes, mosquito and liver stages, consistent with observations that protein export is not restricted to asexual stages. Although amenable to genetic tagging, *HSP101*, *PTEX150*, *EXP2* and *PTEX88* could not be genetically deleted in *Plasmodium berghei*, in keeping with the obligatory role this complex is postulated to have in maintaining normal blood-stage growth. In contrast, the putative thioredoxin-like protein TRX2 could be deleted, with knockout parasites displaying reduced grow-rates, both *in vivo* and *in vitro*, and reduced capacity to cause severe disease in a cerebral malaria model. Thus, while not essential for parasite survival, TRX2 may help to optimize PTEX activity. Importantly, the generation of TRX2 knockout parasites that display altered phenotypes provides a much-needed tool to dissect PTEX function.**

Accepted 17 July, 2013. *For correspondence. E-mail taniad@deakin.edu.au; Tel. (+61) 3 5227 2923; Fax (+61) 3 5227 2615. †Present address: The Walter and Eliza Hall Institute, Melbourne, Vic. 3052, Australia.

Introduction

Malaria remains a global health burden, causing approximately 660 000 deaths and a further 220 million clinical cases annually (World Health Organization, 2012). The clinical symptoms of malaria are associated with the stage when *Plasmodium* parasites reside within red blood cells (RBCs), with *Plasmodium falciparum* responsible for the largest proportion of human symptomatic infection. The pathogenicity of *P. falciparum* is attributable to its remarkable ability to radically remodel its host RBC; a process involving a number of sophisticated mechanisms that lead to the trafficking of hundreds of parasite proteins beyond its encasing parasitophorous vacuole membrane (PVM), with consequential structural and biochemical changes to the host cell (for a review see Maier *et al.*, 2009; Haase and de Koning-Ward, 2010). The diverse roles these exported proteins play include facilitating nutrient and solute exchange as well as presenting adhesion proteins, particularly PfEMP1, on the infected RBC surface (Crabb *et al.*, 1997; Staines *et al.*, 2006; Nguitragool *et al.*, 2011). The latter facilitates binding of the infected RBC to the microvasculature, thereby preventing their clearance from the spleen and additionally leading to the pathologies associated with *Plasmodium* infection (David *et al.*, 1983; Duffy and Fried, 2003; Haldar and Mohandas, 2007).

The discovery of a conserved pentameric PEXEL/HT motif that mediates protein export into the host RBC has enabled the 'exportome' of malaria parasites to be defined (Hiller *et al.*, 2004; Marti *et al.*, 2004). While *P. falciparum* is predicted to export between 300 and 460 proteins, comparison of the orthologous proteins in other *Plasmodium* spp. revealed they possess much smaller exportomes (Marti *et al.*, 2004; Sargeant *et al.*, 2006; van Ooij and Haldar, 2007; van Ooij *et al.*, 2008; Pick *et al.*, 2011; Boddey *et al.*, 2013). One plausible explanation for the larger exportome in *P. falciparum* is the expansion of protein families in this species, including those that contain

Plasmodium helical interspersed subtelomeric (PHIST) family and DnaJ domains (Sargeant *et al*., 2006). Moreover, PfEMP1, which is encoded by ~60 *var* genes (Su *et al*., 1995), is only expressed in *P. falciparum* (Hall *et al*., 2005), and a large percentage of exported proteins additionally contribute to the correct presentation of this molecule on the infected RBC surface (Maier *et al*., 2008). However, more recent studies have revealed non-falciparum species may indeed export a much larger number of proteins than first predicted, including a large repertoire of PEXEL-negative exported proteins (PNEPs) (Di Girolamo *et al*., 2008; Fernandez-Becerra *et al*., 2009; Pain and Hertz-Fowler, 2009; Sijwali and Rosenthal, 2010; Bernabeu *et al*., 2012; Fonager *et al*., 2012; Pasini *et al*., 2012), with the number of putative *Plasmodium berghei* exported proteins now in excess of 350 (Pasini *et al*., 2012). Regardless of the size of their respective exportomes, the presence of a functionally conserved PEXEL motif among *Plasmodium* species (Marti *et al*., 2004; Sargeant *et al*., 2006; MacKenzie *et al*., 2008; Sijwali and Rosenthal, 2010), and the observation that exported proteins are present not only on the infected RBC surface but also in vesicular-like membranous structures in both *P. falciparum* and *P. berghei*-infected RBCs (Curra *et al*., 2011; Fonager *et al*., 2012; Ingmundson *et al*., 2012; Pasini *et al*., 2012; Haase *et al*., 2013) suggest that protein trafficking and host-cell remodelling is conserved among the *Plasmodium* spp. This intimates that exported proteins are trafficked via a common mechanism and, as the export of some proteins are essential to parasite survival (Maier *et al*., 2008; Ingmundson *et al*., 2012; Pasini *et al*., 2012; Haase *et al*., 2013), implies that the core components of the trafficking pathway will represent outstanding targets for chemotherapeutic intervention against all forms of malaria. Drugs that target these proteins should simultaneously block many key proteins that exhibit diverse functions, and thus not surprisingly, there has been considerable interest in dissecting the molecular pathways that facilitate protein export in malaria parasites.

To gain access to the host cell cytosol, exported proteins must initially transverse the PVM. A large macromolecular complex has been identified at this membrane in *P. falciparum* that displays the characteristics predicted for a *P*lasmodium *T*ranslocon of *EX*ported proteins and accordingly has been termed PTEX (de Koning-Ward *et al*., 2009; Gehde *et al*., 2009). PTEX comprises HSP101, PTEX150 and EXP2, and two tentatively assigned components, PTEX88 and TRX2 (de Koning-Ward *et al*., 2009). The latter two proteins still require validation that they are constituents of PTEX as their identity was based on proteomic approaches that were used to identify proteins that co-affinity purified with HSP101 and PTEX150 (de Koning-Ward *et al*., 2009). HSP101 is an AAA^+ATPase (El Bakkouri *et al*., 2010) and is the predicted energy source for protein unfolding prior to translocation through the pore-forming component of PTEX, which is proposed to be EXP2 based on its biochemical and predicted structural properties (de Koning-Ward *et al*., 2009; Bullen *et al*., 2012). The functions of PTEX150 and the putative component PTEX88 remain unknown; orthologues are only found in *Plasmodium* (Aurrecoechea *et al*., 2009). The other putative component TRX2 is a small ~13 kDa protein that belongs to the thioredoxin family of proteins that acts to reduce disulphide bonds in substrate proteins via a conserved CXXC active site (reviewed in Nickel *et al*., 2006). This protein has previously been localized to the mitochondria (Boucher *et al*., 2006), to the PV(M) (Sharma *et al*., 2011) and to an unidentified structure within the parasite and at the PV (Kehr *et al*., 2010).

Given the suspected role of PTEX in protein export and, by association, parasite survival and virulence because certain exported proteins are essential and impart virulent attributes upon the parasite, we were interested in using a genetic approach to determine the consequence of disrupting the function of the PTEX components. We elected to do this in the rodent malaria parasite *P. berghei*, which would allow us to characterize and explore the role of PTEX in pathogenesis and survival *in vivo* across the malaria life cycle. To achieve this, we first needed to confirm that the orthologous PTEX components EXP2, HSP101 and PTEX150 colocalize and exist as a complex in *P. berghei.* Importantly, this provided validation that TRX2 and PTEX88 are indeed genuine components of PTEX. Second, we revealed that PTEX is expressed in other 'zoite' stages of the malaria life cycle, namely salivary gland sporozoites and liver merozoites. As for the blood-stage merozoites, expression at these stages would provide a mechanism for the parasite to insert PTEX into the PVM upon invasion of a new host cell (albeit hepatocyte or RBC) to rapidly facilitate protein export, which in the infected RBC stages begins shortly thereafter (Riglar *et al*., 2013). Finally, attempts to genetically disrupt all five PTEX components in *P. berghei* revealed HSP101, EXP2, PTEX150 and PTEX88 are likely core components of PTEX and hence are attractive drug targets. In contrast, we demonstrate that the fifth component, TRX2, is a non-essential accessory PTEX protein. Nevertheless, the marked growth and virulence phenotypes of parasites lacking TRX2 confirms an important blood-stage role for the PTEX complex and suggests that this protein plays a key regulatory role in PTEX function.

Results

PTEX components are expressed in P. berghei *and exist as a complex*

Orthologues of the five *P. falciparum* PTEX components are found in the genomes of all *Plasmodium* spp.

sequenced to date, including *P. berghei* (Aurrecoechea *et al*., 2009). A schematic showing the distinguishing features of the *P. falciparum* PTEX components and the corresponding proteins in *P. berghei* is presented in Fig. S1.

Prior to determining which of the PTEX protein components are essential to *P. berghei* survival and PTEX function through gene knockout approaches, it was first necessary to establish that these proteins indeed form a similar complex in *P. berghei* and second to provide evidence that TRX2 and PTEX88 are genuine constituents of PTEX. To do this, a series of transgenic *P. berghei* ANKA parasite lines were created in which each of the genes encoding the five endogenous putative *P. berghei* ANKA (Pb) PTEX components were tagged with a triple haemagglutinin (HA)/single streptactin II epitope tag using a 3′ replacement strategy as outlined in Fig. 1A. After positive selection with pyrimethamine, transgenic parasites were isolated and subjected to genotyping by diagnostic PCR. This analysis revealed that for each transgenic line created, the endogenous locus had been modified in the expected manner (Fig. 1B). Appropriate epitope tagging in each line was subsequently confirmed by Western blot analysis of parasite extracts harvested from the blood of infected mice. All species reacting with the anti-HA antibody migrated at approximately the predicted molecular mass of the respective protein, with no labelling observed in control *P. berghei* wild-type (WT) lysates as expected (Fig. 1C). These transgenic parasites are hereafter referred to as Pb101-HA, Pb150-HA, PbEXP2-HA, Pb88-HA and PbTRX2-HA. While additional bands were observed in Pb150-HA lysates, they most likely represent breakdown products of 150-HA since the orthologous protein in *P. falciparum* is also highly susceptible to degradation (T.F. de Koning-Ward, unpublished). Rabbit polyclonal antibodies raised against recombinant *P. falciparum* HSP101 (anti-Pf101) and EXP2 (anti-PfEXP2) (de Koning-Ward *et al*., 2009) also recognized single protein species of the expected molecular mass in *P. berghei* ANKA WT, and correspondingly greater molecular mass proteins in Pb101-HA or PbEXP2-HA parasites, respectively, consistent with the addition of the epitope tags in transgenic parasites and demonstrating that these antibodies cross-react with the orthologous *P. berghei* protein (Fig. 1D). The reactivity of the ~ 26 kDa band in PbEXP2-HA with anti-PfEXP2 indicates the presence of untagged EXP2 in the population (Fig. 1D). Importantly, these data demonstrate that the loci encoding each putative PTEX gene in *P. berghei* are amenable to gene targeting.

Next, immunofluorescence analyses (IFA) was performed to localize the orthologous PTEX proteins in the ring-stages of *P. berghei* ANKA infected RBC (Fig. 2A). Both the anti-PfEXP2 antibody and anti-HA antibody colocalized in fixed smears of PbEXP2-HA, giving the same punctate labelling pattern outside the parasite periphery corroborating that EXP2 had been successfully epitope-tagged in *P. berghei*. This punctate localization is consistent with that observed for *P. falciparum* EXP2. HSP101-HA and PTEX150-HA also clearly colocalized with EXP2, using the anti-EXP2 and anti-HA antibodies (Fig. 2A). Unfortunately, the anti-HSP101 antibody gave non-specific labelling in *P. berghei* ANKA parasites by IFA (data not shown), and could not be used for colocalization studies. These observations are in keeping with EXP2, HSP101 and PTEX150 associating at the PVM in *P. falciparum* (de Koning-Ward *et al*., 2009; Bullen *et al*., 2012). The creation of the transgenic Pb88-HA line also allowed localization of PTEX88 in *Plasmodium* spp. for the first time, revealing that it too colocalized with PbEXP2, providing support that this protein is a PTEX component (Fig. 2A). The localization of TRX2, however, was less clear and made difficult by the fact that expression of TRX2-HA was weak. In the early ring stages we observed some co-labelling of TRX2-HA with EXP2 but more pronounced internal parasite labelling with the anti-HA antibodies (Fig. 2A). As the parasites matured, the localization of TRX2-HA appeared more towards the parasite periphery rather than PV/PVM and its localization within the parasite also more pronounced. It should be noted that *P. falciparum* HSP101 also labels broadly through the parasite across the asexual cell cycle (Riglar *et al*., 2013) but in this instance we could not colocalize TRX2 and HSP101 due the lack of a *P. berghei* HSP101 antibody with utility for IFA. The localization of TRX2-HA within the parasite was not confined to a single structure as previously observed for TRX2-GFP (which was overexpressed from episomes under transcriptional control of a non-native promoter) (Kehr *et al*., 2010) and may represent TRX2-HA that is in the process of being trafficked or recycled, or alternatively may represent an additional functional role for this protein in the parasite. By schizont stages TRX2-HA displayed punctate apical labelling, reminiscent of labelling pattern observed with other PTEX components in *P. falciparum* and Pb150-HA (Fig. 2B).

To definitively resolve whether these five proteins, including TRX2 and PTEX88 form a complex in *P. berghei,* protein lysates derived from the transgenic *P. berghei* parasites expressing HA-tagged versions of the orthologous PTEX components were used in affinity purification experiments with rabbit anti-HA and then probed with either mouse anti-HA (Fig. 3A), anti-Pf101 (Fig. 3B) or anti-EXP2 (Fig. 3C). As expected, anti-HA antibodies specifically pulled-down each of the five HA-tagged proteins, whereas no signal was detected when WT lysate was used as a control (only the control for TRX2-HA is shown in Fig. 3A, bottom panel). In addition, affinity purification of PTEX150-HA and EXP2-HA resulted in the co-precipitation of HSP101 (Fig. 3B), and PTEX150-HA and

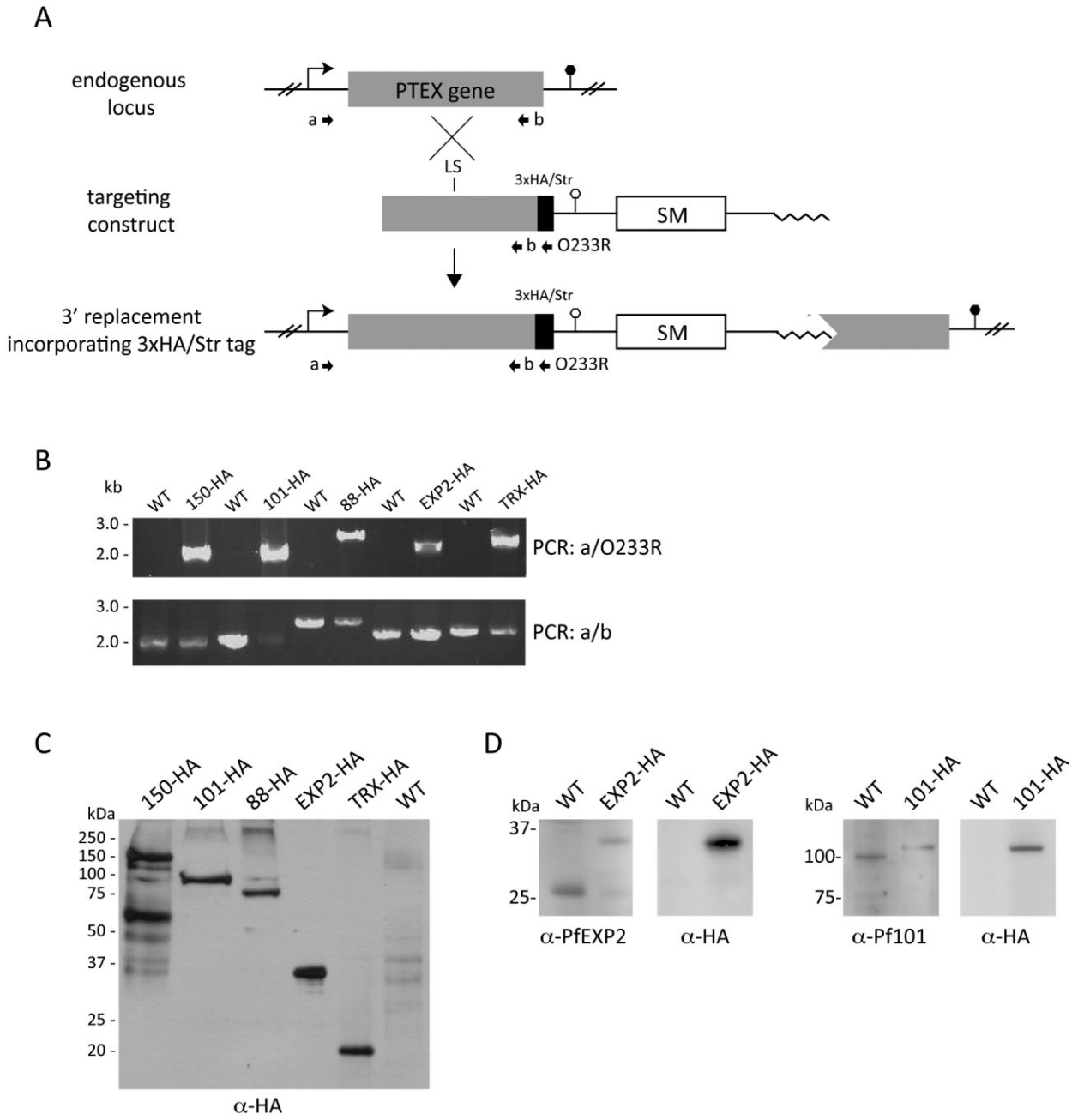

Fig. 1. Generation of *P. berghei* transgenic parasites expressing epitope tags.
A. The targeting constructs were designed to integrate into the respective *P. berghei* PTEX locus by single-crossover recombination, such that the complete open reading frame was reconstituted while simultaneously introducing a combined C-terminal triple haemagglutinin (HA) and single Strep-II (Str) epitope tag. The predicted structure of the endogenous locus before and after 3′ integration is shown. Black box, 3xHA/Str epitope tags; SM, *Toxoplasma gondii* DHFR-TS selectable marker cassette; wavy lines, plasmid backbone; right arrow, transcription start site; circle, transcription terminator; LS, linearization site; arrowheads, oligonucleotides used in diagnostic PCR analysis.
B. Diagnostic PCR to detect integration events. Oligonucleotide combinations a/O233R were used to detect incorporation of the epitope tags into transgenic PbPTEX150 (150-HA), PbHSP101 (101-HA), PbTEX88 (88-HA), PbEXP2 (EXP2-HA) and PbTRX2 (TRX2-HA), whereas oligonucleotide combination a/b PCR up the wild-type (WT) PTEX gene.
C. Western blot analysis of parasite proteins extracted from WT and transgenic *P. berghei* parasites harvested from infected mice using anti-HA antibodies.
D. Western blot analysis of WT and transgenic PbEXP2-HA and Pb101-HA using the indicated antibodies reveal that the anti-PfEXP2 and anti-Pf101 recognize a predominant protein species in WT *P. berghei* extracts of roughly the predicted molecular weight, while slightly higher species are observed in the transgenic parasite lines due to the incorporation of the epitope tags.

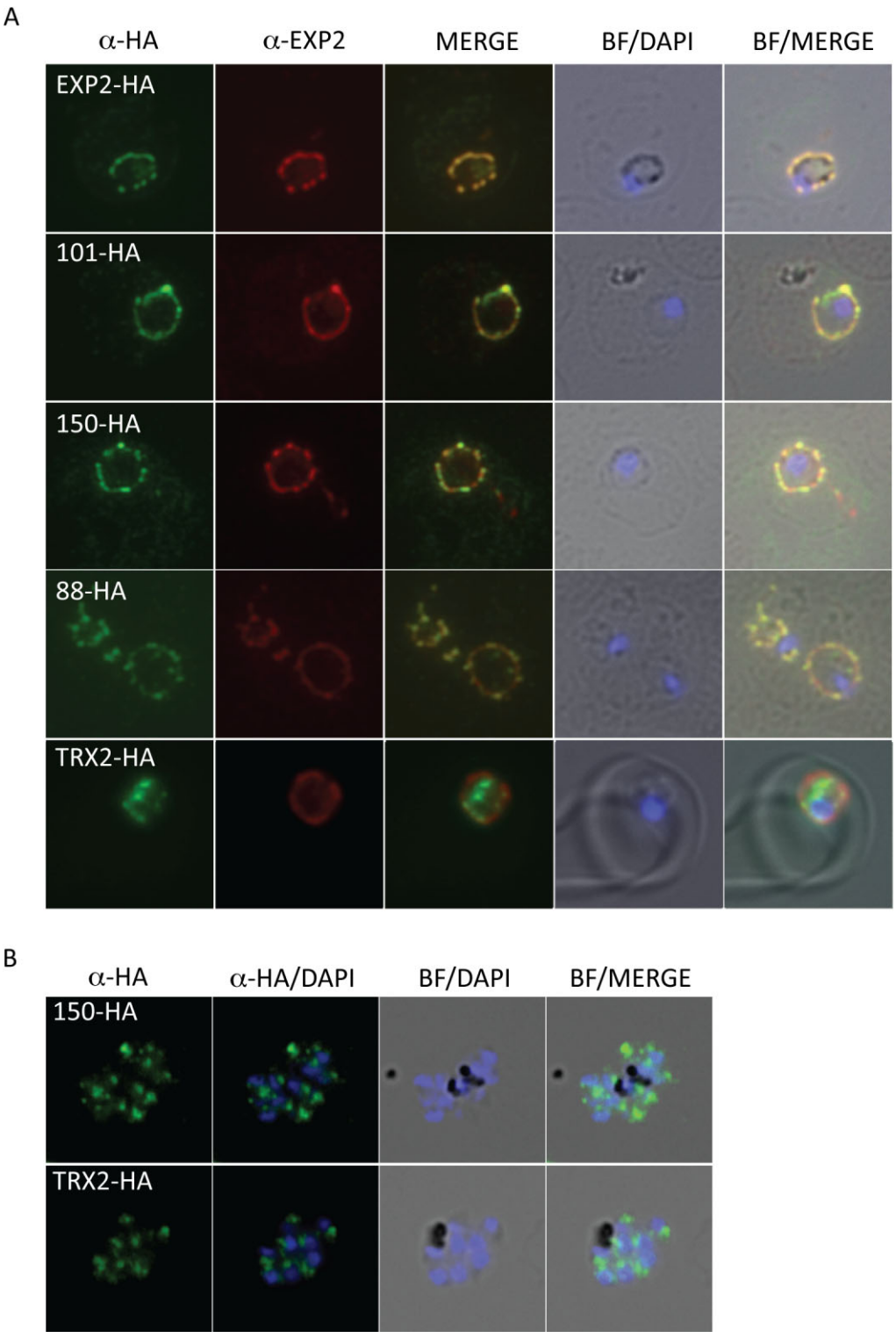

Fig. 2. *P. berghei* PTEX components colocalize and have PV/PVM localization. Double-labelling IFA performed on (A) fixed rings stages or (B) fixed schizont stages of *P. berghei* PTEX-HA transgenic parasites using the antibodies as indicated. The original magnification for all IFA images was ×1000.

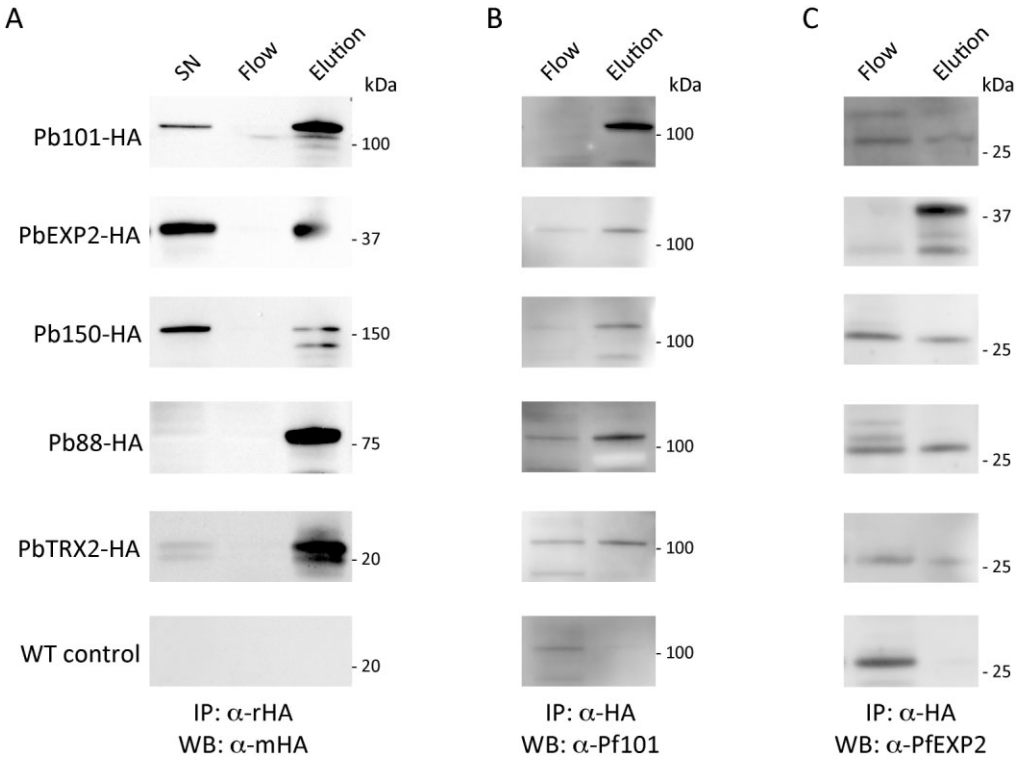

Fig. 3. The five putative PTEX components form a complex in *P. berghei*, including PTEX88 and TRX2. Immunoblot analysis of immunoprecipitations (IP) performed on *P. berghei* ANKA wild-type (WT) and transgenic HA-tagged parasite lysates using anti-HA antibody (α-HA) for the IP and probed with (A) anti-HA, (B) anti-Pf101 or (C) anti-EXP2. Supernatant (SN) was collected after parasite lysate was centrifuged and the flow fraction represents unbound supernatant material. The presence of PTEX components in the elution fraction of immune-precipitations performed on HA-tagged parasites and their absence in the *P. berghei* wild-type (WT) control indicates the interaction is specific. Note that in the uncloned PbEXP2-HA transgenic population the EXP2 antibody detects both epitope-tagged and untagged EXP2 in oligomers that dynamically associate.

HSP101-HA co-precipitated EXP2 (Fig. 3C). These interactions are specific as no signal against HSP101 or EXP2 was detected in the elution fraction when control WT lysate was used in pull-down experiments using anti-HA antibodies (Fig. 3B and C, bottom panel). Importantly, these experiments revealed that TRX2-HA and PTEX88-HA also specifically interacted with HSP101 (Fig. 3B) and EXP2 (Fig. 3C).

As the anti-PfEXP2 and anti-PfHSP101 antibodies reacted rather weakly against *P. berghei* lysate, we obtained additional evidence that TRX2 is a component of PTEX through proteomic approaches. Specifically, proteins from PbTRX2-HA or PbWT control lysates that affinity purified with anti-HA antibodies were separated by SDS-PAGE and gel slices that were suspected to contain proteins that specifically interacted with TRX2-HA were subject to protein identification by capillary liquid chromatography coupled online with tandem mass spectrometry (LC-MS/MS) sequencing. Twenty-seven peptides to PTEX components (including HSP101, EXP2 and PTEX88) were detected in gel slices from the TRX2-HA pull-down (Table S1) whereas no PTEX peptides were detected in the corresponding PbWT pull-down. In contrast, other non-PTEX peptides (ribosomal proteins for example) could be recovered in both the PbWT and TRX2-HA pull-downs. Together, these results confirm the specificity of the PTEX interactions with TRX2.

Further corroboration that PTEX88 is a component of the PTEX complex was also obtained by creating a *P. falciparum* transgenic parasite line in which the C-terminus of PTEX88 is tagged with a triple HA/single streptactin II tag. As can be seen from Fig. 4A, a band corresponding to the expected molecular weight of PTEX88-HA (~ 92.5 kDa) was observed, validating that PTEX88 had been epitope tagged. Interestingly, a lower-molecular-weight band of < 50 kDa was consistently observed; it remains unknown, however, if this lower band represents a degraded or processed form of PTEX88-HA. Although expression of PTEX88-HA in this transgenic line was weak, consistent with the suggestion from proteomics that PTEX88 is in much lower abundance than other PTEX components (de Koning-Ward *et al.*, 2009), it also colocalized with PTEX150 and EXP2 in *P. falciparum* (Fig. 4B). Immunoprecipitation with anti-HA antibodies affinity purified

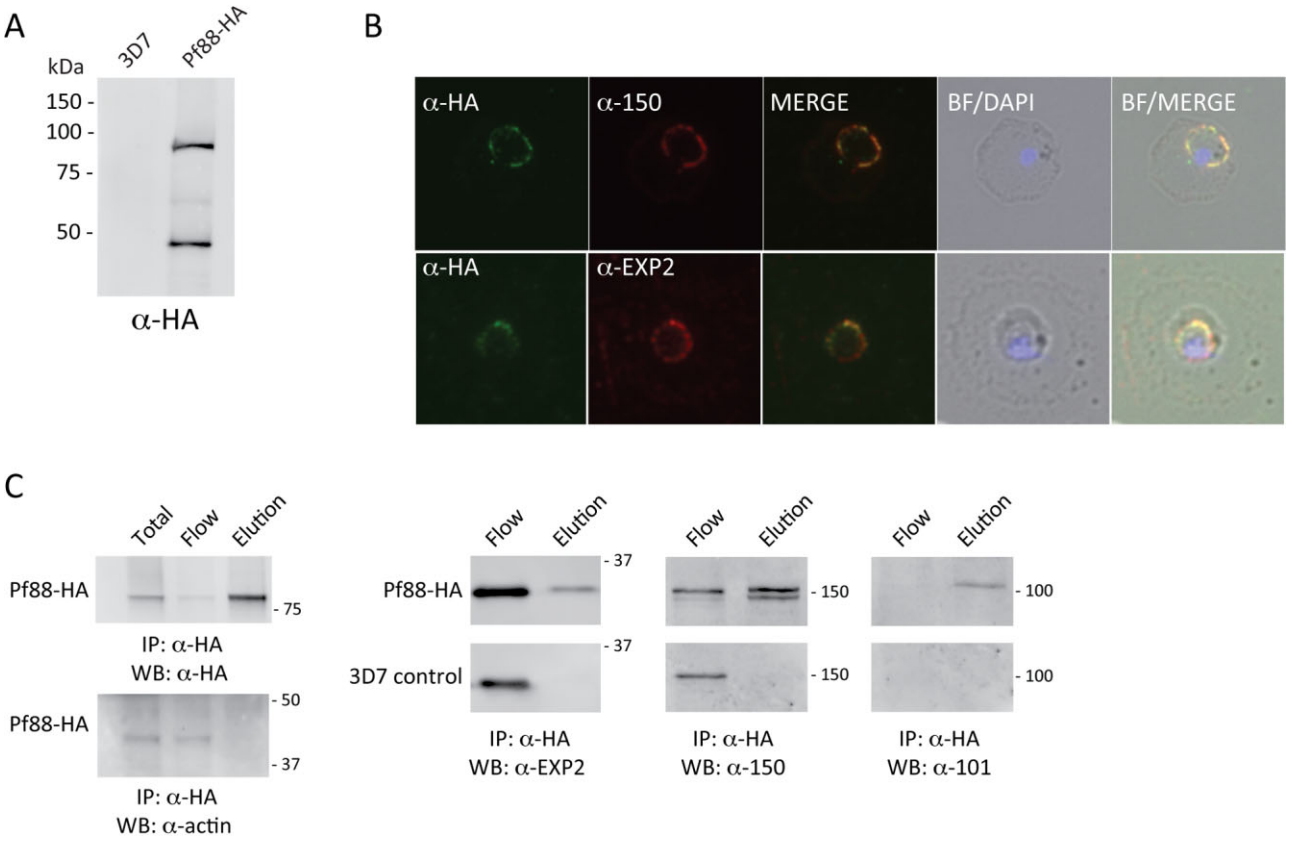

Fig. 4. Epitope tagging of *P. falciparum* PTEX88 confirms its PVM localization and interaction with other PTEX components.
A. Western blot analysis confirming the endogenous *P. falciparum PTEX88* gene has been tagged with a combined triple haemagglutinin (HA) and single Strep-II (Str) epitope tag at the C-terminus.
B. Double-labelling IFA performed on ring stages of *P. falciparum* PTEX88-HA with the antibodies as indicated.
C. Immunoblot analysis of immunoprecipitations performed on PfTEX88-HA using α-HA antibodies shows lack of interaction of PTEX88-HA with a non-PTEX protein (actin), whereas a specific interaction is observed with EXP2, PTEX150 and HSP101 as PTEX components are not detected in the elution fraction of 3D7 control parasites.

PfPTEX88-HA but not actin as expected. Moreover, PfPTEX88-HA affinity purified EXP2 and HSP101 in a specific manner as the corresponding pull-down performed with *P. falciparum* 3D7 WT lysate was negative (Fig. 4C). Taken altogether, the above experiments provide the definitive proof that a PTEX complex exists in *P. berghei* and that PTEX88 and TRX2 are indeed *bona fide* members of this complex.

Targeted disruption of each PTEX gene identifies likely core and accessory components

We next attempted to functionally characterize individual components of the PTEX complex in *P. berghei* by attempting to generate loss-of-function mutants of all five components. For this, linear PTEX targeting vectors were transfected into *P. berghei* ANKA parasites on three separate occasions. These constructs are designed to recombine by double crossover at the 5′ and 3′ targeting sequences, leading to replacement of the endogenous gene with the *Toxoplasma gondii* DHFR-TS drug selectable marker (Fig. S2A and Fig. 5A). After positive selection with the antimalarial drug pyrimethamine, parasites transfected with the HSP101 targeting construct were never recovered, whereas parasites were obtained for PTEX150, EXP2, PTEX88 and TRX2. Genotyping by PCR diagnostic for integration at the 5′ and 3′ ends revealed PTEX150, EXP2 and PTEX88 were refractory to gene deletion in three independent gene knockout attempts (data not shown) and that parasites contained only episomal versions of the targeting construct. These results were confirmed by Southern blot analysis of genomic DNA probed with 5′ or 3′ targeting regions (Fig. S2B). Since the genes encoding HSP101, PTEX150, EXP2 and PTEX88 were all amenable to genetic targeting via 3′-replacement (Fig. 1), their refractoriness to gene deletion indicates that these four PTEX components are likely to be core translocon components whose expression is either essential for para-

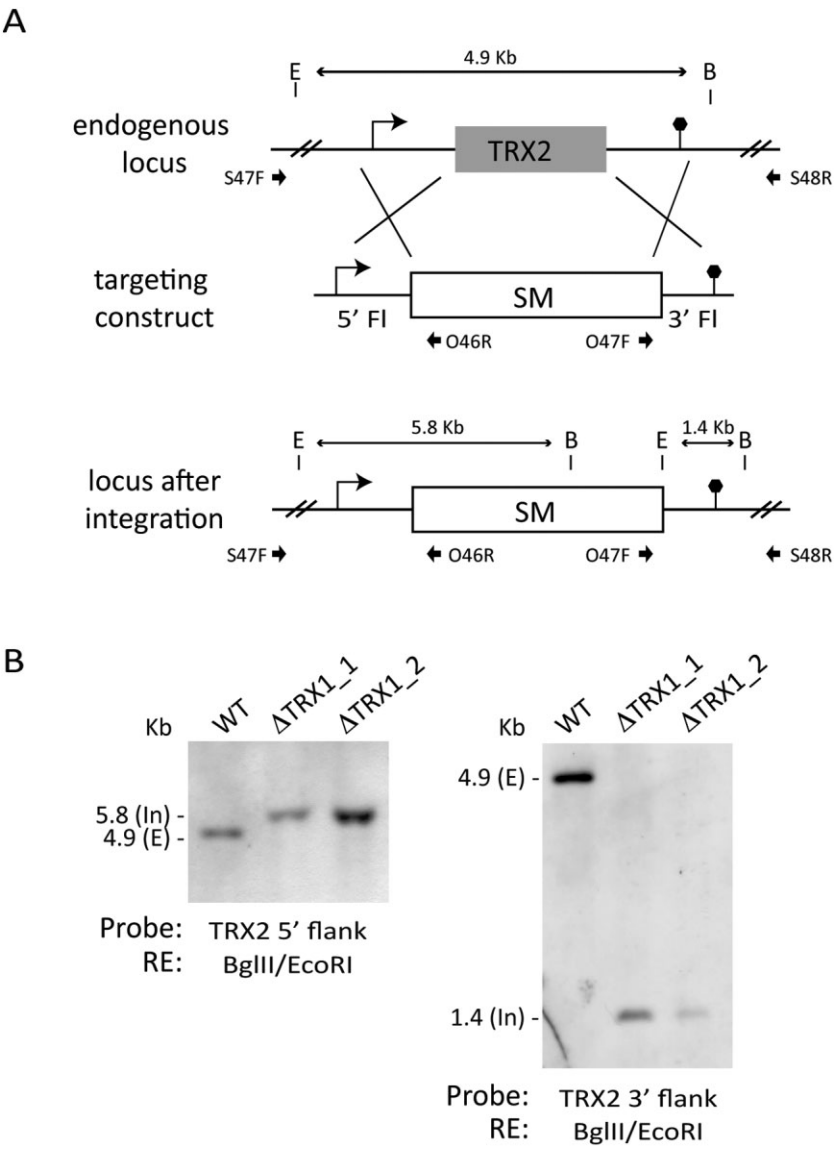

Fig. 5. The *P. berghei TRX2* gene is not essential for parasite survival.
A. The *P. berghei* TRX2 targeting construct was designed to integrate into the endogenous locus by double-crossover recombination. The predicted structure of the endogenous locus before and after integration is shown. 5′ Fl, 5′ targeting sequence; 3′ Fl, 3′ targeting sequence; SM, *Toxoplasma gondii* DHFR selectable marker cassette; right arrow, transcription start site; circle, transcription terminator; arrowheads, oligonucleotides used in diagnostic PCR analysis.
B. Southern blot showing homologous integration into the PbTRX2 gene as predicted. Genomic DNA from the *P. berghei* ANKA wild-type (WT) and two independent ΔPbTRX2 clones digested with restriction enzymes as indicated and probed with either the 5′ or 3′ targeting sequence. In both cases the endogenous locus (E) has been modified and integration bands (In) of the predicted size are seen.

site survival in the blood stages of malaria infection or required to provide a significant advantage in blood-stage growth.

In contrast to the other four components, we were surprised to find that transgenic parasites with a disrupted TRX2 gene (ΔPbTRX2) could be obtained following transfection with the TRX2 targeting construct (Fig. 5A) on two independent occasions. PCRs diagnostic for integration at the 5′ (S47F/O46R) and 3′ (O47F/S48R) ends revealed integration had occurred with subsequent loss of the WT gene (data not shown). Clonal ΔPbTRX2 devoid of wild type contamination were subsequently generated by intravenous injection of limiting dilutions of parasites into mice and two clones from independent transfections were analysed further (ΔPbTRX2_1 and ΔPbTRX2_2). Southern blot analysis of genomic DNA digested with BglII and EcoRI and probed with either the 5′ or the 3′ targeting sequence confirmed loss of the WT gene, as demonstrated by absence of a 4.9 kb band, and appearance of either a 5.8 or a 1.4 kb band, respectively, which correspond to the expected integration event (Fig. 5B).

It was noted that when the ΔPbTRX2 clonal lines were used to infect BALB/c mice for genotyping analysis, these parasites grew consistently slower than WT parasites. Indeed comparative infection experiments of the parasite lines in BALB/c mice confirmed that loss of TRX2 had a significant impact on growth (Fig. 6A). Despite their delayed growth in mice, the ΔPbTRX2 clones were ultimately able to generate high parasite loads, although from day 9 post infection (p.i.), comparative analysis between groups could no longer be accurately performed as mice infected with WT had to be humanely culled due to high

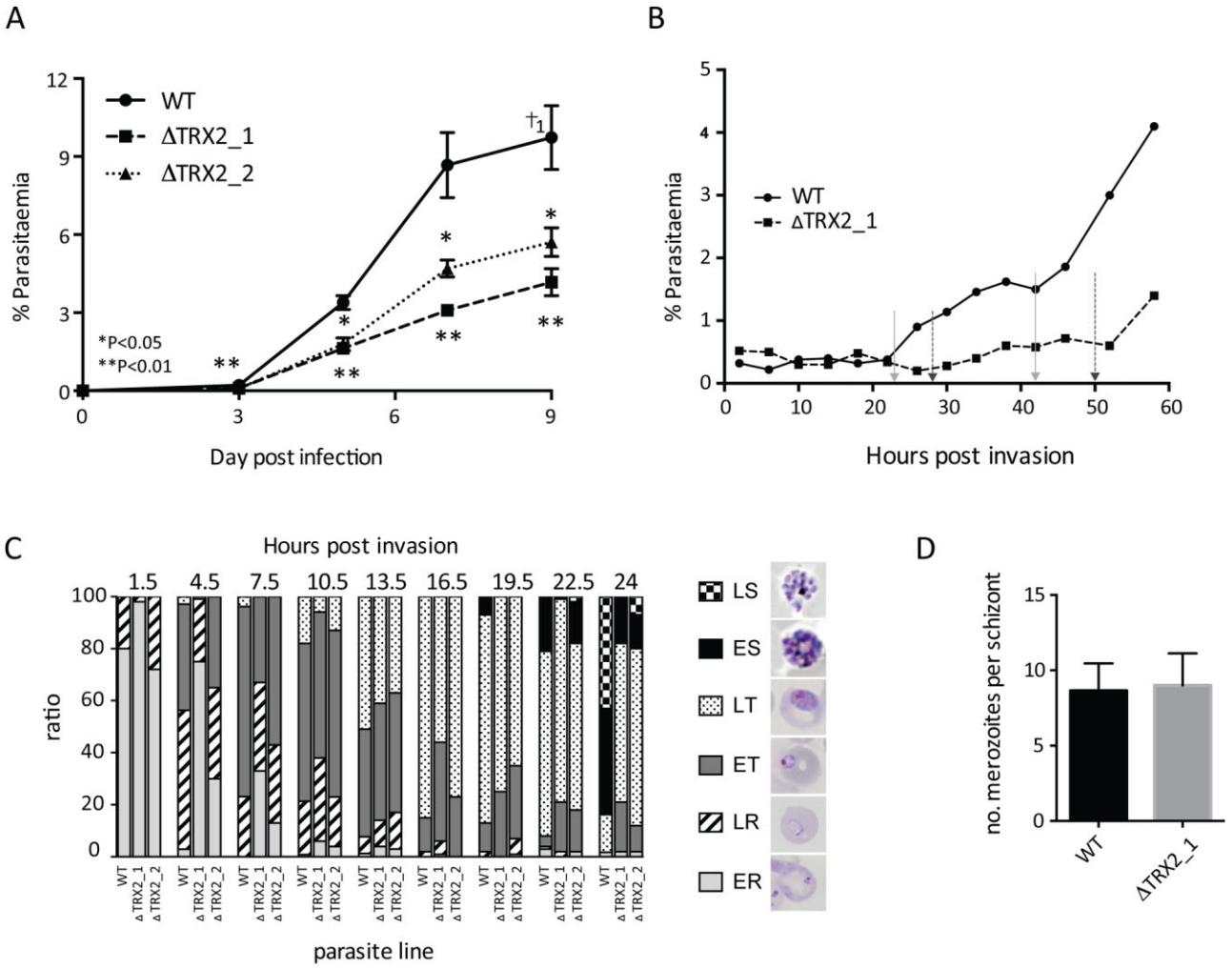

Fig. 6. Loss of TRX2 leads to altered growth phenotypes *in vivo* and *in vitro*.
A. Growth curves of *P. berghei* wild-type (WT) and ΔPbTRX2 clones in BALB/c mice ($n = 12$). The cross indicates number of mouse deaths. Data were pooled from two separate experiments. Error bars represent SEM. A two-tailed Student's *t*-test was used to calculate statistical significance.
B. *In vivo* growth analysis of *P. berghei* parasite lines in which invasion had been synchronized *in vitro* prior to intravenous inoculation in mice. The solid grey and black dashed arrows indicate the time points at which new invasion events of WT and ΔPbTRX2_1, respectively, could be detected.
C. *In vitro* growth analysis of *P. berghei* parasite lines following synchronous invasion *in vitro*. ER, early ring; LR, late ring; ET, early trophozoite; LT, late trophozoite; ES, early schizont; LS, late schizont.
D. Column graph depicting the number of merozoites formed per mature schizont ($n = 50$).

parasite burdens. For example, at day 11 p.i. the percentage parasitaemias were 33.6 ± 4.3, 21.3 ± 3.2 and 24.2 ± 2.4 for WT (45% survival), ΔPbTRX2_1 (100% survival) and ΔPbTRX2_2 (100% survival) respectively.

We reasoned that the growth delay of ΔPbTRX2 clones *in vivo* may have stemmed from an altered cell cycle, or that infected RBC were being cleared more efficiently by the spleen, particularly if TRX2 contributes to the export of virulence proteins that are involved in sequestration. To examine growth further, pure merozoite preparations devoid of contaminating schizonts were added to fresh RBCs and invasion allowed to proceed for 30 min. Infected RBCs were then intravenously administered to mice and blood smears analysed every 2–4 h for the next three cell cycles (Fig. 6B). While newly invaded WT ring-stage parasites were observed 23 h later, ΔPbTRX2_1 took an extra 5 h to reinvade erythrocytes. A similar delay was observed in the second cycle, such that ΔPbTRX2_1 now lagged around 8 h behind the WT parasites. Furthermore, despite similar numbers of infected RBC being administered to mice, the parasitaemias of ΔPbTRX2_1 were less than half that of WT parasites during the second cycle. Repeats of this experiment yielded very similar results (data not shown).

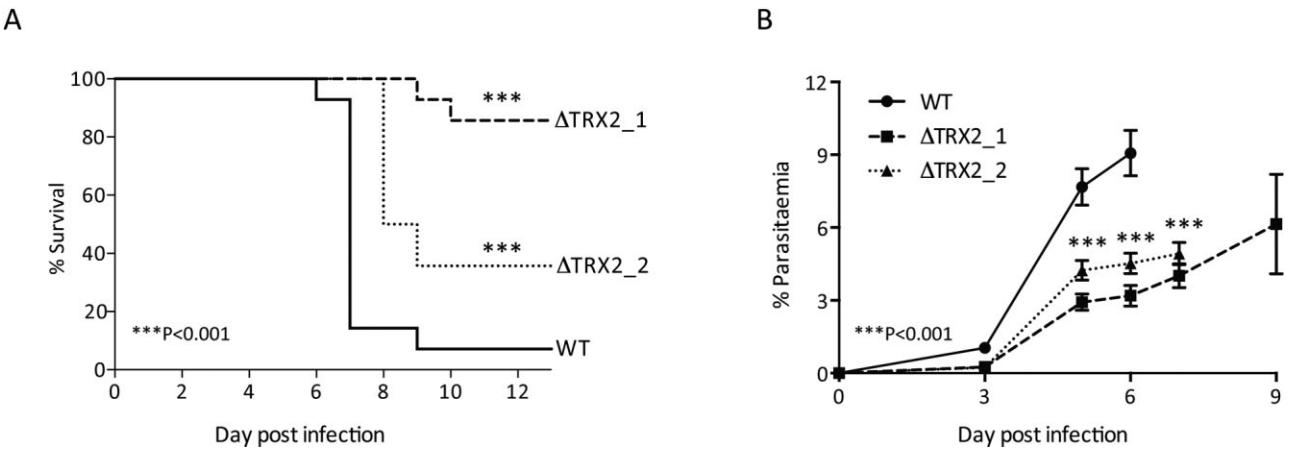

Fig. 7. Loss of TRX2 leads to altered virulence and growth phenotypes in C57/Bl6 mice. (A) Survival curves ($n = 14$) and (B) growth curves of parasite lines ($n = 12$) in C57/Bl6 mice. Data were pooled from two separate experiments. Error bars represent SEM. A two-tailed Student's *t*-test was used to calculate statistical significance.

As trophozoite and schizont stages sequester in the *in vivo* experiments described above, we repeated the *in vitro* invasion but this time continued to culture the parasites *in vitro* until mature schizonts formed to examine more closely what stage of the cell cycle the loss of TRX2 has its greatest impact. The most obvious delays occurred at the beginning and end of the cell cycle (Fig. 6C). At 4.5 h post invasion (p.i.), only 2.9% of WT parasites remained at early ring-stage, whereas 75% of ΔPbTRX2_1 and 30% of ΔPbTRX2_2 were still at this stage. By 7.5 h p.i., the majority of WT had progressed into early trophozoite stage (73%), with no early rings remaining whereas 33% and 13% of ΔPbTRX2_1 and ΔPbTRX2_2, respectively, had still not moved beyond the early ring stage. Likewise, by 24 h p.i. when 83% of the WT parasites had already entered the schizont stage (43% early and 40% late schizonts), only 15% of ΔPbTRX2_1 and 20% of ΔPbTRX2_2 were at a similar stage of parasite development, with low numbers of late schizonts formed, if any. However, examination of the mature schizonts used to prepare the merozoites for the *in vitro* invasion assay did not reveal a difference in the number of merozoites per schizont between the WT and ΔPbTRX2_1 (Fig. 6D).

As PTEX is implicated in the export of virulence proteins and infection of C57/Bl6 mice with *P. berghei* ANKA normally causes a severe lethal form of malaria (termed experimental cerebral malaria or ECM) that is associated with a multitude of neurological symptoms and extensive underlying pathology, we also compared the virulence of WT and ΔPbTRX2 clones in C57/Bl6 mice. Mice infected with WT parasites rapidly succumbed to ECM around day 7 p.i., whereas mice infected with the ΔPbTRX2 clones showed a marked delay in developing ECM, if at all (Fig. 7A). The parasitaemias of the infected C57/Bl6 mice were also examined and the ΔPbTRX2 clones showed delays in parasitaemia similar to what was observed in BALB/c mice (Figs 7B and 6A). While WT mice exhibited a mean parasitaemia of 9.1% ± 0.9 on day 6 p.i. (1 day prior to developing ECM), by day 9 p.i. when all but one WT mouse had been culled, mice infected with ΔPbTRX2_1 exhibited a mean parasitaemia of only 5.0% ± 0.5 (86% survival) and mice that survived infection with ΔPbTRX2_2 (36% survival) had a mean parasitaemia of 5.6% ± 1.6 (Fig. 7B). Moreover, even when the ΔPbTRX2 clones reached higher parasitaemias, this did not influence their ability to cause ECM. Although the ΔPbTRX2 clones varied slightly in their potential to cause ECM and in their growth rates, it is important to note that both clones consistently grew significantly slower and displayed altered virulence when compared with the WT line on all occasions. The reasons for the difference between the lines is unclear but may be related to the number of times the clones had been passaged.

The PTEX components are expressed throughout the malaria life cycle

To date PTEX has been associated with the export of soluble PEXEL-containing proteins in the asexual blood stages (de Koning-Ward *et al.*, 2009); however, PEXEL-containing proteins have also been identified in other stages of the malaria life cycle, namely gametocyte and liver stages (Singh *et al.*, 2007; Silvestrini *et al.*, 2010; Ingmundson *et al.*, 2012). This suggests that PTEX may function at multiple stages of the parasite life cycle. With the *P. berghei* PTEX-HA transgenic parasites in hand created as part of this study, in combination with anti-PfPTEX antibodies, we decided to explore this further.

Initially PTEX expression in *P. berghei* PTEX-HA transgenic parasites that had switched into gametocytes

was examined. Although gametocyte development in *P. berghei* is only slightly longer than the ~ 24 h asexual cycle, mature gametocytes can be readily distinguished from asexual stage parasites in blood smears by their size, pigment and presence of a single nucleus. Surprisingly, PTEX150-HA, HSP101-HA and PTEX88-HA expression was not observed at the PVM in these stages. Moreover, the expression of EXP2 at the PVM and punctate labelling of TRX2-HA within the parasite was weak (Fig. S3). From this we infer that PTEX is not functional at this stage of parasite development. However, in order to explore PTEX expression in gametocytes further, we undertook similar analysis in the *P. falciparum* 3D7 WT strain as gametocyte maturation in this species occurs across a much longer time frame of ~ 9–12 days and so in contrast to *P. berghei*, would enable us to determine if PTEX is present in the early gametocyte stages. For this, antibodies to the early gametocyte marker Pfs16 were used to discriminate between the asexual stages and stage I/II and III gametocytes by IFA, together with the three available *P. falciparum* PTEX antibodies. Figure 8 reveals that EXP2, HSP101 and PTEX150 were all expressed in stage I-III gametocytes, which is also in keeping with the presence of these proteins in the *P. falciparum* stage I-II proteome (Silvestrini *et al.*, 2010). However, already from stage I/II and even more so by stage III, labelling of the PTEX components was observed more towards the parasite periphery and within the gametocyte itself, rather than colocalizing with the PVM protein Pfs16 (Fig. 8). Altogether these combined results suggest that newly synthesized PTEX components in the schizont stages of parasites that are committed to becoming gametocytes are injected into the PV upon merozoite invasion but that by the time the gametocyte has reached stage III of its development, the PTEX machinery has begun to be disassembled. The observation that EXP2 is retained for longer at the PVM of gametocytes is most likely because it has a tighter association with this membrane relative to other PTEX components (Bullen *et al.*, 2012). Indeed by the time the *P. falciparum* gametocytes reach stage V, PTEX labelling is only observed within the parasite (data not shown). Our findings also correlate with the observed enrichment of gametocyte-specific exported proteins in stage1-II gametocyte proteomes and their depletion in mature stage V gametocytes (Silvestrini *et al.*, 2010).

We also examined the expression of PTEX components during the sporozoite and late liver stages of the *P. berghei* life cycle. Since PTEX150 and EXP2 had already been shown in a recent study to be present at the PVM of *P. falciparum* infected hepatocytes in mice engrafted with human hepatocytes (Vaughan *et al.*, 2012), the rationale for looking at the sporozoite and liver merozoites stems from the fact that in the asexual stages PTEX is already synthesized in merozoites to ensure that PTEX can be rapidly assembled in the new host cell after parasite invasion to facilitate early protein export (Riglar *et al.*, 2013). Accordingly, we wanted to examine the analogous stages in the infected mosquito/liver. RT-PCR performed on RNA extracted from mosquitoes and hepatocytes infected with *P. berghei* ANKA WT parasites revealed that PTEX components were transcribed in midgut sporozoites and also in late liver stages coinciding with when parasites were undergoing schizogony (Fig. 9A). Transcription of EXP2 in particular was also observed at earlier time points of both stages of development (oocyts and 24–48 h liver). This was not unexpected since EXP2 is not co-regulated with HSP101 and PTEX150 in the asexual stages, despite ending up with these components in the dense granules of merozoites and the PVM of ring stages (Bullen *et al.*, 2012). It was surprising to find, however, two different PTEX150 transcript sizes in the liver stages as this has not been observed previously in the asexual stages and the significance of this will require further follow up. The expression of PTEX components was also examined by IFA on salivary glands sporozoites extracted from mosquitoes infected with PbANKA, Pb101-HA or Pb150-HA using anti-PfEXP2 or anti-HA antibodies. This analysis demonstrated EXP2, HSP101 and PTEX150 were all expressed in this invasive parasite form (Fig. 9B). Likewise, multiple punctate staining for EXP2, HSP101 and PTEX150 was also observed in individual merozoites in the late liver stages, which upon release into the bloodstream, would go on to invade erythrocytes (Fig. 9C). Thus our combined results are consistent with the proposal that PTEX is contained within invasive 'zoite' stages of the malaria life cycle to facilitate rapid assembly of PTEX at the PVM of a newly invaded host cell, whether that is an erythrocyte or hepatocyte, in order to facilitate protein export. A compilation of all of the experimental evidence for PTEX expression throughout the malaria life cycle, obtained through our own experiments as outlined herein, as well as from other studies is presented in Table S2.

Discussion

PTEX was originally identified in *P. falciparum* using a range of proteomic, biochemical and cell biological approaches (de Koning-Ward *et al.*, 2009). That analysis and a subsequent study by Bullen *et al.* (2012) revealed PTEX comprises of PTEX150, HSP101 and EXP2, in addition to two tentatively assigned constituents, TRX2 and PTEX88 (de Koning-Ward *et al.*, 2009; Bullen *et al.*, 2012). In this study we provide evidence through the creation of novel transgenic *P. berghei* and *P. falciparum* lines in conjunction with reciprocal immunoprecipitation experiments that PTEX88 and TRX2 are indeed *bona fide* members of PTEX. It should be noted that although the localization of TRX2 has not been completely resolved, the

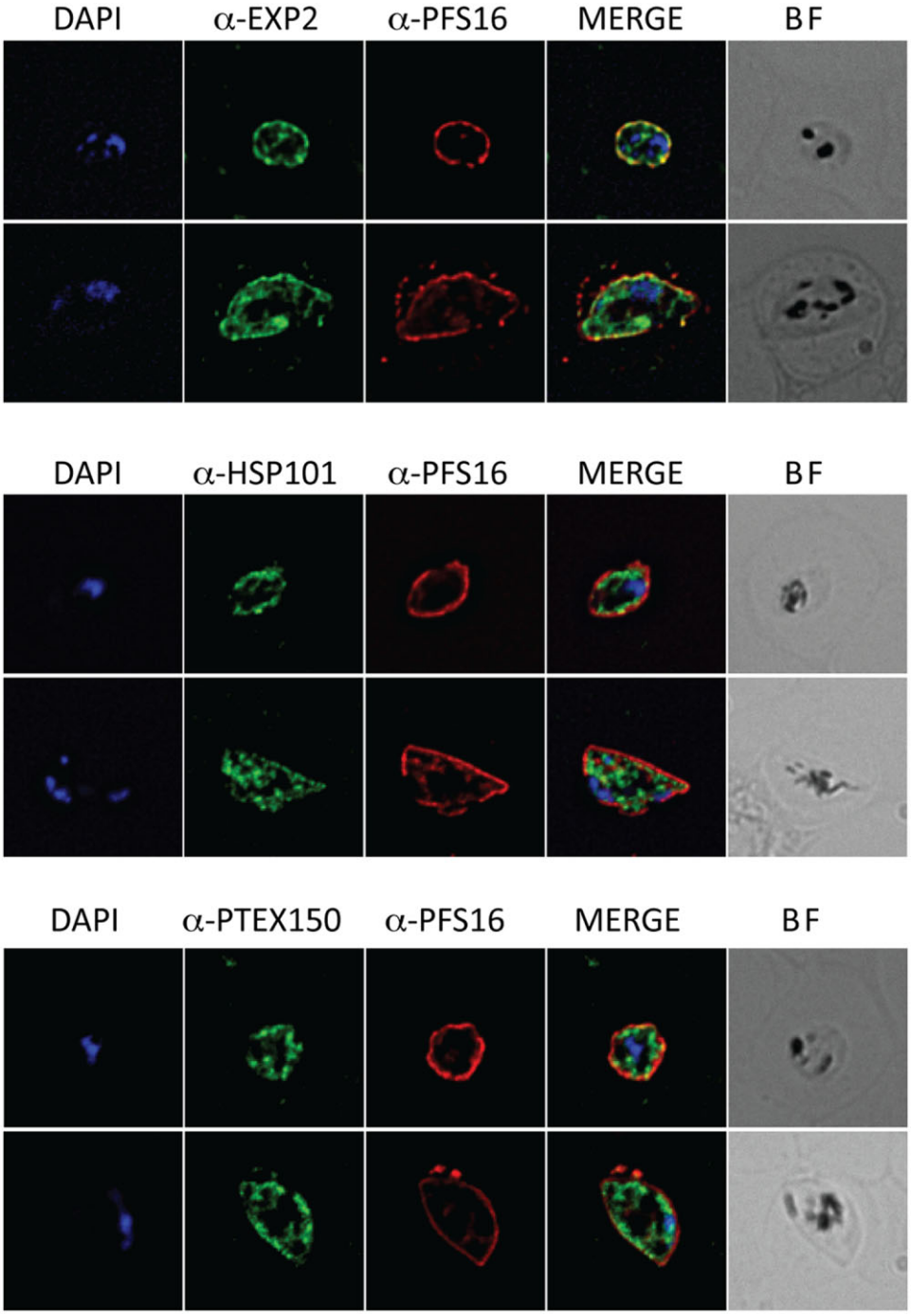

Fig. 8. PTEX is expressed in stage I/II gametocytes but undergoes degradation during gametocyte maturation. Double-labelling IFA performed on fixed *P. falciparum* 3D7 gametocytes using the antibodies as indicated. Pfs16 is an integral gametocyte-specific PVM protein expressed from stages I/II of *P. falciparum* gametocytes. Gametocytes in the top panel are stage I/II gametocytes, whereas those in the bottom panel are at stage III.

finding that it is expressed in schizonts and present during early ring stages at either the PV/PVM (Kehr *et al.*, 2010; Sharma *et al.*, 2011) is not inconsistent with having a role in PTEX function. Whether the presence of TRX2 at other locations infers a function additional to PTEX is unknown, although our mass spectrometry analysis of proteins that affinity purified with TRX2-HA has so far failed to yield any obvious proteins that suggests this may be the case.

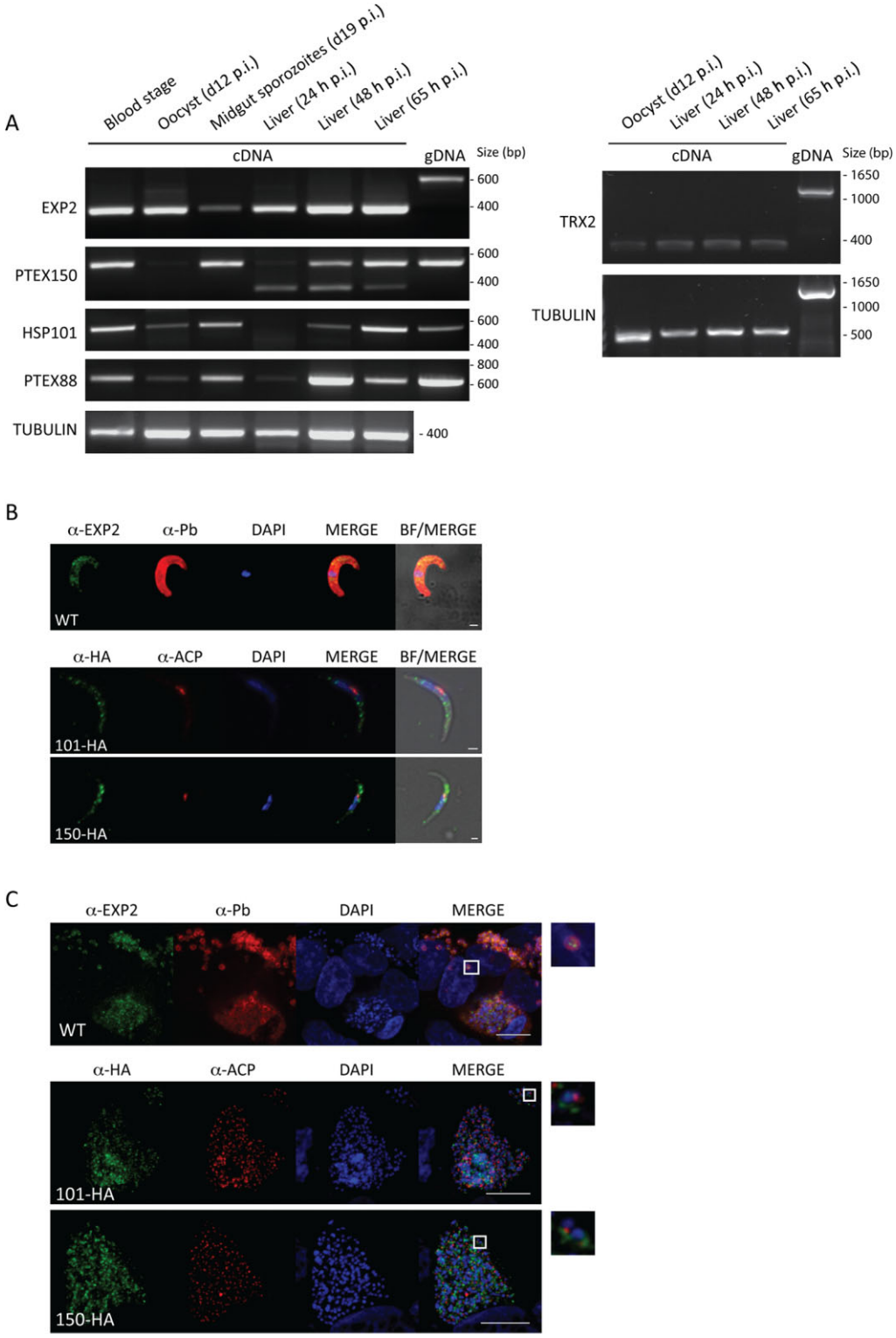

Fig. 9. PTEX is expressed during mosquito and liver stages of parasite development.
A. RT-PCR of PTEX genes and tubulin (loading control) on blood, mosquito (oocyst and midgut sporozoites) and liver stages of parasite development. As controls, genomic DNA (gDNA) isolated from *P. berghei* was also used in PCR.
B and C. (B) Double-labelling IFA performed on fixed salivary gland sporozoites, and (C) infected hepatocytes (~ 68–72 h p.i.), using the antibodies as indicated, including anti-Pb (which recognizes the parasite surface) or anti-ACP (which recognizes the apicoplast). An enlargement of the boxed region showing an individual merozoite is shown to the right. Scale bars represent 1 μm for the sporozoites and 10 μM for the infected hepatocytes.

We also revealed that expression of PTEX is not restricted to just the asexual stages of parasite development and this is in keeping with the observation that PEXEL-containing proteins are also present at other life cycle stages. The proteome of stage I and II *P. falciparum* gametocytes has divulged the identity of at least 26 gametocyte PEXEL-containing proteins that are putatively exported, of which PfMdv-1/Peg3 and Pfg14_0744 have been confirmed as present in the RBC cytosol (Eksi *et al*., 2005; Furuya *et al*., 2005; Silvestrini *et al*., 2010). All components of PTEX are also present in this proteome, with the exception of PTEX88 (Silvestrini *et al*., 2010). This is again in agreement with our own proteome analysis that suggests PTEX88 is in much lower abundance than other PTEX components (de Koning-Ward *et al*., 2009). Our IFA results that show expression of PTEX components in stage I/II gametocytes are also consistent with the gametocyte proteome data. However, it appears that at least HSP101 and PTEX150 are already beginning to dissociate from the PVM during the early gametocyte stages as indicated by lack of colocalization with the integral PVM protein Pfs16 and this in turn is in keeping with an apparent lack of exported proteins in the mature gametocyte proteome (Silvestrini *et al*., 2010).

For the liver stages of parasite development, there is conflicting evidence as to whether export of proteins into the hepatocyte cytosol is PEXEL-mediated (Singh *et al*., 2007; Cockburn *et al*., 2011). While it is plausible that *Plasmodium* parasites can usurp the hepatocyte trafficking machinery to export its proteins into this host cell, the expression of PTEX components in salivary gland sporozoites (this study) and at the PVM in *P. falciparum* infected hepatocytes in mice engrafted with human hepatocytes liver-chimeric mice (Vaughan *et al*., 2012) suggests that at least some parasite proteins may translocate into the host cell via this parasite-derived machinery. However, this remains to be formally proven. The expression of PTEX components in salivary gland sporozoites and merozoites of late liver stages is also analogous to the synthesis of PTEX components in blood-stage merozoites, providing a mechanism for the parasite to insert PTEX into the PVM upon invasion of a new host cell to rapidly facilitate protein export.

The epitope-tagging of PTEX components in *P. berghei* not only confirmed these five components form a complex in this *Plasmodium* spp., importantly it also validated that each PTEX locus is amenable to gene targeting. Hence, as the genes encoding HSP101, PTEX150, PTEX88 and EXP2 could not be disrupted, it is likely they either are all essential or are at least required to significantly enhance parasite growth and survival. Based on the prediction that HSP101 provides the crucial energy source for protein unfolding prior to translocation through the putative pore-forming component, EXP2, it was not unexpected that HSP101 and EXP2 are essential *Plasmodium* proteins. In fact, their essentiality formed one of the initial criteria for their inclusion as a putative PTEX component (de Koning-Ward *et al*., 2009), although for these components it was not formally proven. The lack of orthologues and distinctive protein domains for PTEX150 and PTEX88 outside the *Plasmodium* genus, and the inability to generate gene knockouts precludes assignment of their function at this stage. Nonetheless, based on the make-up of other translocon systems in prokaryotes and eukaryotes, which usually comprise chaperones, receptors and structural components, in addition to the pore-forming component and the molecular motor (Schnell and Hebert, 2003), we envisage that PTEX150 and PTEX88 most likely serve as structural components of PTEX or potentially act as a receptor for the cargo to dock prior to translocation across the PVM.

In contrast, it was surprising that TRX2 could be successfully disrupted in *P. berghei*, with knockout lines demonstrating both growth and virulence phenotypes. The reduced growth rates *in vivo* do not appear to be the result of fewer merozoites produced per schizont. Rather, ΔPbTRX2 parasites took longer to progress through the cell cycle (as indicated by both *in vitro* and *in vivo* experiments) and fewer ΔPbTRX2 parasites also made it through each cycle *in vivo*. Whether this is a result of some parasites dying each cycle due to poorer nutrient uptake for example or from greater clearance of infected RBC through the spleen awaits further investigation. Interestingly, the most obvious growth delays of the ΔPbTRX2 parasites occurred during schizont and ring stages, which correlates with when TRX2 is first expressed and when PTEX is predicted to be functional respectively.

Although repeated attempts to genetically complement ΔPbTRX2 parasites by using a second selectable marker were unsuccessful (probably due to the initial poor health and growth of the ΔPbTRX2 parasites), it should be noted that both independent ΔPbTRX2 clones consistently demonstrated similar phenotypes in each assay. Unfortunately, the ability to examine the export phenotypes of the ΔPbTRX2 clones by transfection of chimeric exported (versus non-exported) GFP reporter constructs has also been unsuccessful due to the same reasons and only recently have *P. berghei* PEXEL-containing proteins been identified and demonstrated to be exported. Thus, although the functional proof that TRX2 and the PTEX machinery facilitates protein export will require further experimentation that is outside the scope of this study, we can infer from these results that TRX2 is an accessory component of PTEX. Other translocons also comprise non-essential accessory components (Schnell and Hebert, 2003), which help to regulate activities such as translocon assembly, its status in an open/closed configuration, and the translocation of particular proteins under

certain conditions. Interestingly, both chloroplasts and mitochondria use redox signals to regulate protein translocation across their respective membranes (for a review see Stengel *et al.*, 2010). For example, in chloroplasts, redox signals modulate the formation and reduction of inter- and intra-molecular disulphide bonds of translocon components at the outer membrane to regulate protein import. Additionally, the redox state of the stroma is sensed by the translocon at the inner chloroplast membrane and when there is a high demand for redox-related proteins, the efficiency of translocation of this subset of proteins is adjusted accordingly (Stengel *et al.*, 2009; 2010). As EXP2 and PTEX88 harbour numerous conserved cysteine residues (Fig. S1), PTEX could also be redox regulated to adjust protein export into the host cell cytosol; TRX2 is the most obvious candidate to perform this function. Since some of the exported proteins are predicted to be involved in nutrient uptake, this could account for the ΔPbTRX2 clones exhibiting reduced growth rates. Alternatively, TRX2 may regulate the export of a particular subset of cysteine-rich proteins that are not essential for parasite survival but aid parasite virulence. To date, only soluble exported proteins have been associated with PTEX (de Koning-Ward *et al.*, 2009), and to our knowledge this class of proteins in *Plasmodium* spp. do not contain cysteine residues. However, it remains to be ascertained whether PTEX also aids in the translocation of cysteine-rich transmembrane-containing proteins found in the infected host cell such as the RIFIN, STEVOR and PfMC-2TM superfamily of proteins (Lavazec *et al.*, 2006). Thus, by determining the substrates of TRX2, the putative function(s) of this thioredoxin in the PTEX complex may ultimately be revealed.

In conclusion, as the PTEX constituents are expressed at multiple stages of the parasite life cycle and are putatively required for the export of hundreds of parasite-derived proteins into host cells, they are likely to provide outstanding targets for anti-malaria chemotherapeutic intervention. Despite the finding that TRX2 is an accessory PTEX component and thus should no longer be considered a suitable drug target (Sharma *et al.*, 2011), its thioredoxin activity, the role of redox signals in other translocon systems, and the ability to alter TRX2 expression without causing parasite lethality all provide a much needed segue for future studies aimed at unravelling how PTEX functions.

Experimental procedures

Ethics statement

All experiments involving rodents were performed in strict accordance with the recommendations of the Australian Government and National Health and Medical Research Council Australian code of practice for the care and use of animals for scientific purposes. The protocols were approved by the Animal Welfare Committee at Deakin University (Approval No.: AWC A97/10 and A98/2010) and Melbourne University (Approval No.: AEC 1212488).

Plasmid constructs

To create the vectors that were used to epitope tag the endogenous *P. berghei* ANKA (Pb) PTEX genes, the following cloning procedures were performed. First ~ 2 kb immediately upstream of the stop codon of PbPTEX150 (which would ultimately serve as the targeting region for homologous recombination into the PbTEX150 endogenous locus) was PCR-amplified from *P. berghei* ANKA genomic DNA (gDNA) in roughly two equal parts using the oligonucleotides O34F/O35R (5′ targeting region) and O36F/O37R (3′ targeting region) (refer to Table S3 for oligonucleotide sequences). By sewing the two resulting PCR products together with O34F/O37R, this created a SpeI site between the two adjacent 5′ and 3′ sequences that would later be used to linearize the DNA prior to transfection. The sewn PCR product was then digested with NotI and PstI and cloned in place of the *P. falciparum* PTEX150 in pTEX150-HA/Str 3′ (de Koning-Ward *et al.*, 2009). Subsequent digestion with NotI and EcoRV excised the PbTEX150-HA/Str sequence together with the downstream *P. berghei* DHFR-TS 3′ UTR and, after treatment with Klenow, was cloned into the pB3 vector (Waters *et al.*, 1997) that had been digested with ClaI and treated with Klenow. As the backbone of this resulting vector contained a SpeI site, this was removed by digestion with NaeI and EcoRV that flank this site, followed by re-ligation of the plasmid, to give the final epitope tagging construct termed pB3-150-HA/Str-DT3′. From this vector all subsequent *P. berghei* PTEX tagging constructs were made by replacement of the PbTEX150 5′ and 3′ targeting regions using SacII/SpeI and SpeI/AvrII, respectively, with the targeting sequences of HSP101 (amplified using O38F/O39R and O40F/O41R), TRX2 (O42F/O43R and O44F/O45R), PTEX88 (O46F/O47R and O48F/O49R) and EXP2 (MK13F/MK14R and MK15F/MK16R). Prior to transfection into *P. berghei* ANKA parasites, all targeting constructs were linearized with SpeI to drive integration into the endogenous PTEX locus.

For targeted gene deletion of the PTEX genes, fragments of the 5′ UTR and 3′ UTR that would serve as targeting regions to drive integration into the endogenous locus (de Koning-Ward *et al.*, 2000) were PCR-amplified from *P. berghei* ANKA gDNA using gene-specific primers for HSP101 (S23F/S24R and S25bF/S26bR), EXP2 (S9F/S10R and S11F/S12R), PTEX88 (S1F/S2R and S3F/S4R) and TRX2 (S5F/S6R and S7F/S8R). The 5′ UTR homologous sequences were digested with ApaI/SacII (or HindIII/SacII in the case of the PTEX88 5′ UTR), with the SacII site filled in with Klenow, and cloned into the pB3 vector that was digested with ClaI, treated with Klenow and then digested with ApaI. The 3′ UTR targeting sequences of HSP101 (digested with EcoRV/NotI), EXP2 (EcoRV/SmaI), PTEX88 (EcoRV/EcoRI) and TRX2 (EcoRI/SpeI) were cloned into either the corresponding sites of pB3 containing the respective 5′ UTR or in the case of EXP2 and TRX2 3′ UTRs, into the SpeI site that had been treated with Klenow. The resulting constructs were linearized with KpnI/NotI and used to transfect *P. berghei* ANKA parasites.

To epitope tag the endogenous *P. falciparum* PTEX88 gene, the last ~ 1 kb of the PTEX88 gene minus the stop codon was PCR-amplified from *P. falciparum* 3D7 genomic DNA using the oligonucleotides MK46F/MK47R. The resulting fragment was digested with NotI/PstI and cloned in place of the *P. falciparum* PTEX150 in pTEX150-HA/Str 3′ (de Koning-Ward *et al*., 2009).

Parasites and transfection

The reference clone15cy1 from the *P. berghei* ANKA strain was used to generate all transgenic parasite lines. Transfection of parasites and selection of the transgenic parasites was performed as previously described (Janse *et al*., 2006). Briefly, nycodenz purified *P. berghei* schizonts were prepared for transfection and DNA constructs were introduced using the Nucleofector® electroporation device (Amaxa). The resulting DNA mixture was injected intravenously into 6- to 8-week-old BALB/c mice and drug selection with pyrimethamine (0.07 mg ml^{-1}) of genetically transformed parasites begun at day 1 post transfection. Clonal lines of the ΔPbTRX2 parasites were generated by intravenous injection of limiting dilutions of parasites into naïve mice.

Blood-stage *P. falciparum* 3D7 were cultured continuously and transfected as previously described (Trager and Jensen, 1976; Crabb *et al*., 2004). Gametocyte cultures were initiated as described in Dearnley *et al*. (2012). Briefly, trophozoite stage parasites at 2% parasitaemia were rapidly expanded. In the following cycle, the 8–10% trophozoites were then subdivided to 2% trophozoites in 5% haematocrit. Following reinvasion (day 0), the cultures were maintained in the presence of 62.5 mM *N*-acetyl glucosamine to inhibit asexual replication. Giemsa-stained slides were used to monitor stage progression. The medium was changed daily but no fresh erythrocytes were added. Stage I–II gametocytes were harvested on day 2–4 of culture.

Anopheles stephensi mosquitoes were infected with *P. berghei* by feeding on infected mice. Midguts were dissected from mosquitoes 12–14 days post feeding to collect midgut sporozoites and salivary gland sporozoites were isolated from salivary glands. Coverslips seeded with 2×10^5 HepG2 liver cells were grown for 18 h and then infected with 15 000–20 000 sporozoites per well. Where required, growth medium was replaced 2 h p.i. and at 24 h intervals thereafter.

Nucleic acid analysis

The genotypes of ΔPbTRX2 clonal lines were confirmed by Southern blot analysis of gDNA isolated from infected blood. Nucleic acid probes were synthesized using the DIG PCR Probe Synthesis kit. Detection was performed using the DIG Luminescent Detection kit (Roche) according to the manufacturer's protocol. To detect PTEX transcripts in *P. berghei* ANKA parasites by RT-PCR, RNA was extracted from blood, mosquito and liver-stage parasites, using the NucleoSpin™ RNA II Kit (Macherey&Nagel) followed by DNase I (Invitrogen) treatment. cDNA was then made using the Omniscript™ RT Kit (Qiagen) according to the manufacturers manual (incubation at 37°C for 1 h). cDNA was used in PCR reactions using the oligonucleotide combinations: MK22/MK23 (PbEXP2), MK26/MK27 (PbPTEX88), MK28/MK29 (PbPTEX150), MK40/MK41 (PbHSP101), PbTRX2F/PbTRX2R (PbTRX2) and PbTubulinS/PbTublinAS or DO216F/DO217R (PbTubulin). Each RT-PCR was also performed in the absence of reverse transcriptase to test RNA samples for gDNA contamination.

Indirect IFA

For immunofluorescence microscopy, infected erythrocytes were fixed with ice-cold 90% acetone/10% methanol for 2 min, or with 0.01%/4% gluteraldehyde/para-formaldehyde followed by 0.25% Triton X-100 permeabilization prior to blocking in 1% BSA/PBS. Sporozoites were applied to BSA or poly-L-lysine-coated coverslips and allowed to settle for 10 min. Sporozoites and infected liver cells were fixed for 20 min with 4% paraformaldehyde and permeabilized with ice-cold methanol. *P. falciparum* gametocyte fixation was performed with 100% acetone. All antibody incubations were performed in 0.5% BSA/PBS, with the exception of sporozoite and liver cell culture and *P. falciparum* gametocyte IFAs, where incubations were performed in 3% BSA/PBS. Primary antibodies for *P. berghei* blood stages were used at the following concentrations: rabbit anti-EXP2 (1:500), rabbit anti-HSP101 (1:300), rat anti-HA (1:300). For liver and sporozoite stages, rabbit anti-EXP2 was used at 1:250, rat anti-HA at 1:100, anti-PfACP at 1:500 and mouse polyclonal anti-*P. berghei* at 1:500. For *P. falciparum* these antibodies, in addition to rabbit anti-PTEX150 and mouse anti-Pfs16, were used at 1:1000. After three washes with mouse tonicity PBS, the appropriate Alexa Fluor 488/568-conjugated secondary antibodies were used at 1:4000 (Molecular Probes) with DAPI (0.5 μg ml^{-1}). Images were acquired with an Olympus IX70, Leica TCS SP2 or DeltaVision Elite microscope and images were processed using NIH ImageJ version 1.47d (http://rsbweb.nih.gov/ij/) or Adobe CS6 Photoshop.

Protein analysis and immunoprecipitations

Infected rodent blood was depleted of leucocytes by passage through a CF11 column (Whatman) and then lysed using 0.02% saponin for 15 min on ice, followed by centrifugation at 20 000 *g* for 5 min. After three washes with ice-cold mouse tonicity (MT) PBS containing 1× complete protease inhibitors (Roche), the parasite pellet was resuspended in 1× reducing sample buffer. For immunoblots, *P. berghei* parasite lysates were separated on a 4–12% gradient SDS-PAGE gels (Invitrogen) and transferred onto 0.45um PVDF membrane (Millipore) using SDS transfer buffer with methanol and a wet transfer blotting device (Bio-Rad). Immunoreactions were performed using antibodies in 3% BSA/PBS and detection was performed using SuperSignal enhanced chemiluminescence (Thermo Fischer Scientific).

For immunoprecipitations (IP), *P. berghei* infected RBCs depleted of leucocytes or *P. falciparum* infected RBC were lysed with 0.02% saponin. Pelleted parasite material (~ 200–300 μg) was lysed with either IP lysis buffer (Pierce) or 0.5% Triton X-100 in PBS containing complete protease inhibitors (Roche). After a 30 min incubation on ice, the material was passed 10 times through a 29G insulin needle, followed by

centrifugation at 21 000 *g* for 10 min at 4°C. The supernatant was affinity purified with either goat anti-HA antibodies coupled to magnetic beads (Miltenyi Biotec Australia) as per the manufacturer's instruction or 150 µl anti-HA sepharose (Roche) for 8 h at 4°C. Unbound material was collected and beads then washed four times with 1 ml lysis buffer and once with 1 ml PBS. Bound proteins were eluted with 50 µl 1× reducing sample buffer and separated by SDS-PAGE.

For immuno-immune-detection primary antibodies used were monoclonal mouse anti-HA (12CA5) (1:1000) (Roche), polyclonal rabbit anti-HSP101 (1/200 for *P. berghei*, 1/500 for *P. falciparum*), monoclonal mouse anti-HSP101 (1/500), polyclonal rabbit anti-PTEX150 (1:200 for *P. falciparum*), monoclonal mouse anti-EXP2 (mAb 7.7, a gift from J. McBride and described previously; Johnson *et al*., 1994) (1/500 for *P. berghei* and 1:2000 for *P. falciparum*). Secondary antibodies were horseradish peroxidase-conjugated goat anti-mouse and goat anti-rabbit antibodies (1:2000, Jackson IR).

Gel excision, in-gel digestion and Nano-LC-MS/MS

Protein spots or bands were manually excised from preparative SDS-PAGE gels and subjected to manual in-gel reduction, alkylation and tryptic digestion. All gel samples were reduced with 10 mM DTT for 30 min, alkylated for 30 min with 50 mM iodoacetic acid and digested with 375 ng trypsin (Promega) for 16 h at 37C. The extracted peptide solutions were then acidified (0.1% formic acid) and concentrated to approximately 10ul by centrifugal lyophilization using a SpeedVac AES 1010 (Savant). Extracted peptides were injected and fractionated by nanoflow reversed-phase liquid chromatography on a nano-UHPLC system (Easy *n*-LC II, Thermo Fisher, USA) using a nanoAcquity C18 150 mm × 0.15 mm I.D. column (Waters, USA) developed with a linear 60 min gradient with a flow rate of 250 nl min^{-1} from 100% solvent A (0.1% Formic acid in Milli-Q water) to 100% solvent B (0.1% Formic acid, 60% acetonitrile, (Thermo Fisher, USA) 40% Milli-Q water). The nano UHPLC was coupled online to an LTQ-Orbitrap mass spectrometer equipped with a nanoelectrospray ion source (Thermo Fisher, USA) for automated MS/MS. Up to five most intense ions per cycle were fragmented and analysed in the linear trap, with target ions already selected for MS/MS being dynamically excluded for 3 min.

Mass spectra database searching

For protein identification of gel samples LC-MS/MS data were searched against a non-redundant protein decoy database comprising sequences from the latest version of LudwigNR (Human, Bovine, *P. falciparum* species), as well as their reverse sequences (249275 entries). Mass spectra peak lists were extracted using extract-msn as part of Bioworks 3.3.1 (Thermo Fisher Scientific) linked into Mascot Daemon (Matrix Science, UK). The parameters used to generate the peak lists for the LTQ Orbitrap were as follows: minimum mass 400; maximum mass 5000; grouping tolerance 0.01 Da; intermediate scans 1; minimum group count 1; 10 peaks minimum and total ion current of 100. Peak lists for each nano-LC-MS/MS run were used to search MASCOT v2.2.04 search algorithm (Matrix Science, UK) provided by the Australian Proteomics Computational Facility (http://www.apcf.edu.au). The search parameters consisted of carboxymethylation of cysteine as a fixed modification (+58 Da, for gel samples only), with variable modifications set for NH_2-terminal acetylation (+42 Da) and oxidation of methionine (+16 Da). A precursor mass tolerance of 20 ppm, #13C defined as 1, fragment ion mass tolerance of ± 0.8 Da, and an allowance for up to three missed cleavages for tryptic searches was used.

Parasite growth curves

To assess whether transgenic parasites were affected in their growth and/or replication in comparison with WT parasites, three groups of BALB/c mice were infected with asynchronous 1×10^5 *P. berghei* ANKA WT ($n = 14$) or ΔPbTRX2-infected RBC ($n = 14$). The parasitaemia from each mouse was calculated on a daily basis from 3 days p.i. Mice were humanely culled when parasitaemias exceeded 25%.

Analysis of parasite virulence

As a measure of parasitic virulence, transgenic parasites were compared with WT parasites in their ability to cause cerebral malaria in C57Bl/6 mice. For this, three groups of six C57Bl/6 female mice at 6 weeks of age were infected with 1×10^6 *P. berghei* ANKA WT, ΔPbTRX2_1 or ΔPbTRX2_2 parasites. The parasitaemias from each mouse was calculated from 3 days p.i. and thereafter on a daily basis. Mice were checked every 4 h for cerebral malaria symptoms including ataxia and inability to self-right from day 5 p.i. Mice were culled at the sign of cerebral malaria symptoms or when the parasitaemia exceeded 25%. Statistical analysis was performed using a two-tailed Student's *t*-test.

In vitro *and* in vivo *growth analysis of parasites*

Infected erythrocytes from BALB/C mice were cultured in complete RPMI medium supplemented with 25% FCS overnight at 36.5°C. Schizonts were burst by mechanical action using a fine needle syringe. Purification of viable merozoites was achieved by filtration through a 0.2 µm filter, resulting in a pure population of free merozoites. These were then combined with reticulocyte rich blood obtained from phenylhydrazine pre-treated mice. Invasion was allowed to proceed for 30 min at 37°C with vigorous shaking, upon which the cells continued to be cultured *in vitro* or alternatively they were intravenously injected into naïve mice and monitored by blood smears at 2–4 h intervals.

Statistical analysis

Graphs were generated and data analysed using GraphPad Prism 6.0b Software (MacKiev). Statistical analysis was performed using a two-tailed Student's *t*-test. A P value < 0.05 was considered significant.

Acknowledgements

We thank the Australian Red Cross for red blood cells. This work was supported by grants from the Australian National

Health and Medical Research Council (533811) and Deakin University's Central Research Grants Scheme. M.K. acknowledges support from the Alfred Deakin Fellowship scheme. M.W.A.D. is an NHMRC Early Career Fellow. G.I.McF. is supported by a Program Grant from the NHMRC and a Discovery Grant from the Australian Research Council. T.F.d.K.-W. is supported by an NHMRC Career Development Fellowship.

References

Aurrecoechea, C., Brestelli, J., Brunk, B.P., Dommer, J., Fischer, S., Gajria, B., *et al.* (2009) PlasmoDB: a functional genomic database for malaria parasites. *Nucleic Acids Res* **37:** D539–D543.

Bernabeu, M., Lopez, F., Ferrer, M., Martin-Jaular, L., Razaname, A., Corradin, G., *et al.* (2012) Functional analysis of *Plasmodium vivax* VIR proteins reveals different subcellular localizations and cytoadherence to the ICAM-1 endoethelial receptor. *Cell Microbiol* **14:** 386–400.

Boddey, J.A., Carvalho, T.G., Hodder, A.N., Sargeant, T.J., Sleebs, B.E., Marapana, D., *et al.* (2013) Role of plasmepsin V in export of diverse protein families from the *Plasmodium falciparum* exportome. *Traffic* **14:** 532–550.

Boucher, I.W., McMillan, P.J., Gabrielsen, M., Akerman, S.E., Brannigan, J.A., Schnick, C., *et al.* (2006) Structural and biochemical characterization of a mitochondrial peroxiredoxin from *Plasmodium falciparum*. *Mol Microbiol* **61:** 948–959.

Bozdech, Z., Llinas, M., Pulliam, B.L., Wong, E.D., Zhu, J., and DeRisi, J.L. (2003) The transcriptome of the intraerythrocytic developmental cycle of *Plasmodium falciparum*. *PLoS Biol* **1:** E5.

Bullen, H.E., Charnaud, S.C., Kalanon, M., Riglar, D.T., Dekiwadia, C., Kangwanrangsan, N., *et al.* (2012) Biosynthesis, localisation and macromolecular arrangement of the *Plasmodium falciparum* translocon of exported proteins; PTEX. *J Biol Chem* **287:** 7871–7884.

Cockburn, I.A., Tse, S.W., Radtke, A.J., Srinivasan, P., Chen, Y.C., Sinnis, P., *et al.* (2011) Dendritic cells and hepatocytes use distinct pathways to process protective antigen from *Plasmodium in vivo*. *PLoS Pathog* **7:** e1001318.

Crabb, B.S., Cooke, B.M., Reeder, J.C., Waller, R.F., Caruana, S.R., Davern, K.M., *et al.* (1997) Targeted gene disruption shows that knobs enable malaria-infected red cells to cytoadhere under physiological shear stress. *Cell* **89:** 287–296.

Crabb, B.S., Rug, M., Gilberger, T.W., Thompson, J.K., Triglia, T., Maier, A.G., *et al.* (2004) Transfection of the human malaria parasite *Plasmodium falciparum*. *Methods Mol Biol* **270:** 263–276.

Curra, C., Pace, T., Franke-Fayard, B.M., Picci, L., Bertuccini, L., and Ponzi, M. (2011) Erythrocyte remodeling in *Plasmodium berghei* infection: the contribution of SEP family members. *Traffic* **13:** 388–399.

David, P.H., Hommel, M., Miller, L.H., Udeinya, I.J., and Oligino, L.D. (1983) Parasite sequestration in *Plasmodium falciparum* malaria: spleen and antibody modulation of cytoadherence of infected erythrocytes. *Proc Natl Acad Sci USA* **80:** 5075–5079.

Dearnley, M.K., Yeoman, J.A., Hanssen, E., Kenny, S., Turnbull, L., Whitchurch, C.B., *et al.* (2012) Origin, composition, organization and function of the inner membrane complex of *Plasmodium falciparum* gametocytes. *J Cell Sci* **125:** 2053–2063.

Di Girolamo, F., Raggi, C., Birago, C., Pizzi, E., Lalle, M., Picci, L., *et al.* (2008) *Plasmodium* lipid rafts contain proteins implicated in vesicular trafficking and signalling as well as members of the PIR superfamily, potentially implicated in host immune system interactions. *Proteomics* **8:** 2500–2513.

Duffy, P.E., and Fried, M. (2003) *Plasmodium falciparum* adhesion in the placenta. *Curr Opin Microbiol* **6:** 371–376.

Eksi, S., Haile, Y., Furuya, T., Ma, L., Su, X., and Williamson, K.C. (2005) Identification of a subtelomeric gene family expressed during the asexual-sexual stage transition in *Plasmodium falciparum*. *Mol Biochem Parasitol* **143:** 90–99.

El Bakkouri, M., Pow, A., Mulichak, A., Cheung, K.L., Artz, J.D., Amani, M., *et al.* (2010) The Clp chaperones and proteases of the human malaria parasite *Plasmodium falciparum*. *J Mol Biol* **404:** 456–477.

Fernandez-Becerra, C., Yamamoto, M.M., Vencio, R.Z., Lacerda, M., Rosanas-Urgell, A., and del Portillo, H. (2009) *Plasmodium vivax* and the importance of subtelomeric multigene *vir* superfamily. *Trends Parasitol* **25:** 44–51.

Fischer, K., Marti, T., Rick, B., Johnson, D., Benting, J., Baumeister, S., *et al.* (1998) Characterization and cloning of the gene encoding the vacuolar membrane protein EXP-2 from *Plasmodium falciparum*. *Mol Biochem Parasitol* **92:** 47–57.

Florens, L., Washburn, M.P., Raine, J.D., Anthony, R.M., Grainger, M., Haynes, J.D., *et al.* (2002) A proteomic view of the *Plasmodium falciparum* life cycle. *Nature* **419:** 520–526.

Fonager, J., Pasini, E.M., Braks, J.A., Klop, O., Ramesar, J., Remarque, E.J., *et al.* (2012) Reduced CD36-dependent tissue sequestration of *Plasmodium*-infected erythrocytes is detrimental to malaria parasite growth *in vivo*. *J Exp Med* **209:** 93–107.

Furuya, T., Mu, J., Hayton, K., Liu, A., Duan, J., Nkrumah, L., *et al.* (2005) Disruption of a *Plasmodium falciparum* gene linked to male sexual development causes early arrest in gametocytogenesis. *Proc Natl Acad Sci USA* **102:** 16813–16818.

Gehde, N., Hinrichs, C., Montilla, I., Charpian, S., Lingelbach, K., and Przyborski, J.M. (2009) Protein unfolding is an essential requirement for transport across the parasitophorous vacuolar membrane of *Plasmodium falciparum*. *Mol Microbiol* **71:** 613–628.

Haase, S., and de Koning-Ward, T.F. (2010) New insights into protein export in malaria parasites. *Cell Microbiol* **12:** 580–587.

Haase, S., Hanssen, E., Matthews, K., Kalanon, M., and de Koning-Ward, T.F. (2013) The exported protein PbCP1 localises to cleft-like structures in the rodent malaria parasite *Plasmodium berghei*. *PLoS ONE* **8:** e61482.

Haldar, K., and Mohandas, N. (2007) Erythrocyte remodeling by malaria parasites. *Curr Opin Hematol* **14:** 203–209.

Hall, N., Karras, M., Raine, J.D., Carlton, J.M., Kooij, T.W., Berriman, M., *et al.* (2005) A comprehensive survey of the

Plasmodium life cycle by genomic, transcriptomic, and proteomic analyses. *Science* **307:** 82–86.

Hiller, N.L., Bhattacharjee, S., van Ooij, C., Liolios, K., Harrison, T., Lopez-Estrano, C., *et al*. (2004) A host-targeting signal in virulence proteins reveals a secretome in malarial infection. *Science* **306:** 1934–1937.

Ingmundson, A., Nahar, C., Brinkmann, V., Lehmann, M.J., and Matuschewski, K. (2012) The exported *Plasmodium berghei* protein IBIS1 delineates membranous structures in infected red blood cells. *Mol Microbiol* **83:** 1229–1243.

Janse, C., Franke-Fayard, B., and Waters, A.P. (2006) High-efficiency transfection and drug selection of genetically transformed blood stages of the rodent malaria parasite *Plasmodium berghei*. *Nat Protoc* **1:** 614–623.

Johnson, D., Günther, K., Ansorge, I., Benting, J., Kent, A., Bannister, L., *et al*. (1994) Characterization of membrane proteins exported from *Plasmodium falciparum* into the host erythrocyte. *Parasitology* **109:** 1–9.

Kehr, S., Sturm, N., Rahlfs, S., Przyborski, J.M., and Becker, K. (2010) Compartmentation of redox metabolism in malaria parasites. *PLoS Pathog* **6:** e1001242.

de Koning-Ward, T.F., Janse, C.J., and Waters, A.P. (2000) The development of genetic tools for dissecting the biology of malaria parasites. *Annu Rev Microbiol* **54:** 157–185.

de Koning-Ward, T.F., Gilson, P.R., Boddey, J.A., Rug, M., Smith, B.J., Papenfuss, A.T., *et al*. (2009) A newly discovered protein export machine in malaria parasites. *Nature* **459:** 945–949.

Lavazec, C., Sanyal, S., and Templeton, T.J. (2006) Hypervariability within the Rifin, Stevor and Pfmc-2TM superfamilies in *Plasmodium falciparum*. *Nucleic Acids Res* **34:** 6696–6707.

Le Roch, K.G., Zhou, Y., Blair, P.L., Grainger, M., Moch, J.K., Haynes, J.D., *et al*. (2003) Discovery of gene function by expression profiling of the malaria parasite life cycle. *Science* **301:** 1503–1508.

MacKenzie, J.J., Gomez, N.D., Bhattacharjee, S., Mann, S., and Haldar, K. (2008) A *Plasmodium falciparum* host-targeting motif functions in export during blood stage infection of the rodent malarial parasite *Plasmodium berghei*. *PLoS ONE* **3:** e2405.

Maier, A.G., Rug, M., O'Neill, M.T., Brown, M., Chakravorty, S., Szestak, T., *et al*. (2008) Exported proteins required for virulence and rigidity of *Plasmodium falciparum*-infected human erythrocytes. *Cell* **134:** 48–61.

Maier, A.G., Cooke, B.M., Cowman, A.F., and Tilley, L. (2009) Malaria parasite proteins that remodel the host erythrocyte. *Nat Rev Microbiol* **7:** 341–354.

Marti, M., Good, R.T., Rug, M., Knuepfer, E., and Cowman, A.F. (2004) Targeting malaria virulence and remodeling proteins to the host erythrocyte. *Science* **306:** 1930–1933.

Nguitragool, W., Bokhari, A.A., Pillai, A.D., Rayavara, K., Sharma, P., Turpin, B., *et al*. (2011) Malaria parasite *clag3* genes determine channel-mediated nutrient uptake by infected red blood cells. *Cell* **145:** 665–677.

Nickel, C., Rahlfs, S., Deponte, M., Koncarevic, S., and Becker, K. (2006) Thioredoxin networks in the malarial parasite *Plasmodium falciparum*. *Antioxid Redox Signal* **8:** 1227–1239.

van Ooij, C., and Haldar, K. (2007) Protein export from *Plasmodium* parasites. *Cell Microbiol* **9:** 573–582.

van Ooij, C., Tamez, P., Bhattacharjee, S., Hiller, N., Harrison, T., Liolios, K., *et al*. (2008) The malaria secretome: from algorithms to essential function in blood stage infection. *PLoS Pathog* **4:** e1000084.

Pain, A., and Hertz-Fowler, C. (2009) *Plasmodium* genomics: latest milestone. *Nat Rev Microbiol* **7:** 180–181.

Pasini, E.M., Braks, J.A., Fonager, J., Klop, O., Aime, E., Spaccapelo, R., *et al*. (2012) Proteomic and genetic analysis demonstrate that *Plasmodium berghei* blood stages export a large and diverse repertoire of proteins. *Mol Cell Proteomics* **12:** 426–448.

Pick, C., Ebersberger, I., Spielmann, T., Bruchhaus, I., and Burmester, T. (2011) Phylogenomic analyses of malaria parasites and evolution of their exported proteins. *BMC Evol Biol* **11:** 167.

Riglar, D.T., Rogers, K.L., Hanssen, E., Turnbull, L., Bullen, H.E., Charnaud, S.C., *et al*. (2013) Spatial association with PTEX complexes defines regions for effector export into *Plasmodium falciparum*-infected erythrocytes. *Nat Commun* **4:** 1415.

Sargeant, T.J., Marti, M., Caler, E., Carlton, J.M., Simpson, K., Speed, T.P., *et al*. (2006) Lineage-specific expansion of proteins exported to erythrocytes in malaria parasites. *Genome Biol* **7:** R12.

Schnell, D.J., and Hebert, D.N. (2003) Protein translocons: multifunctional mediators of protein translocation across membranes. *Cell* **112:** 491–505.

Sharma, A., Sharma, A., Dixit, S., and Sharma, A. (2011) Structural insights into thioredoxin-2: a component of malaria parasite protein secretion machinery. *Sci Rep* **1:** 179.

Sijwali, P.S., and Rosenthal, P.J. (2010) Functional evaluation of *Plasmodium* export signals in *Plasmodium berghei* suggests multiple modes of protein export. *PLoS ONE* **5:** e10227.

Silvestrini, F., Lasonder, E., Olivieri, A., Camarda, G., van Schaijk, B., Sanchez, M., *et al*. (2010) Protein export marks the early phase of gametocytogenesis of the human malaria parasite *Plasmodium falciparum*. *Mol Cell Proteomics* **9:** 1437–1448.

Singh, A.P., Buscaglia, C.A., Wang, Q., Levay, A., Nussenzweig, D.R., Walker, J.R., *et al*. (2007) *Plasmodium* circumsporozoite protein promotes the development of the liver stages of the parasite. *Cell* **131:** 492–504.

Staines, H.M., Ashmore, S., Felgate, H., Moore, J., Powell, T., and Ellory, J.C. (2006) Solute transport via the new permeability pathways in *Plasmodium falciparum*-infected human red blood cells is not consistent with a simple single-channel model. *Blood* **108:** 3187–3194.

Stengel, A., Benz, J.P., Buchanan, B.B., Soll, J., and Bolter, B. (2009) Preprotein import into chloroplasts via the Toc and Tic complexes is regulated by redox signals in *Pisum sativum*. *Mol Plant* **2:** 1181–1197.

Stengel, A., Benz, J.P., Soll, J., and Bolter, B. (2010) Redox-regulation of protein import into chloroplasts and mitochondria: similarities and differences. *Plant Signal Behav* **5:** 105–109.

Su, X.-Z., Heatwole, V.M., Wertheimer, S.P., Guinet, F., Herrfeldt, J.A., Peterson, D.S., *et al*. (1995) The large

diverse gene family *var* encodes proteins involved in cytoadherence and antigenic variation of *Plasmodium falciparum*-infected erythrocytes. *Cell* **82:** 89–90.
Tarun, A.S., Peng, X., Dumpit, R.F., Ogata, Y., Silva-Rivera, H., Camargo, N., *et al*. (2008) A combined transcriptome and proteome survey of malaria parasite liver stages. *Proc Natl Acad Sci USA* **105:** 305–310.
Trager, W., and Jensen, J. (1976) Human malaria parasites in continuous culture. *Science* **193:** 673–675.
Vaughan, A.M., Mikolajczak, S.A., Wilson, E.M., Grompe, M., Kaushansky, A., Camargo, N., *et al*. (2012) Complete *Plasmodium falciparum* liver-stage development in liver-chimeric mice. *J Clin Invest* **122:** 3618–3628.
Waters, A.P., Thomas, A.W., van Dijk, M.R., and Janse, C.J. (1997) Transfection of malaria parasites. *Methods* **13:** 134–147.
World Health Organization (2012) World Malaria Report.

Supporting information

Additional supporting information may be found in the online version of this article at the publisher's web-site.